European Journal of Medicinal Chemistry 224 (2021) 113720

Contents lists available at ScienceDirect

European Journal of Medicinal Chemistry

journal homepage: http://www.elsevier.com/locate/ejmech

Development of FABP4/5 inhibitors with potential therapeutic effect on type 2 Diabetes Mellitus

Yu-Long He [a, 1], Meng-Ting Chen [b, c, 1], Ting Wang [b], Ming-Ming Zhang [a], Ying-Xia Li [a, **], He-Yao Wang [b, ***], Ning Ding [a, *]

[a] School of Pharmacy, Fudan University, Shanghai, 201203, China
[b] State Key Laboratory of Drug Research, Shanghai Institute of Materia Medica, Chinese Academy of Sciences, Shanghai, 201203, China
[c] University of Chinese Academy of Sciences, Beijing, 100049, China

ARTICLE INFO

Article history:
Received 20 May 2021
Received in revised form
11 July 2021
Accepted 23 July 2021
Available online 24 July 2021

Keywords:
Type 2 diabetes mellitus
Dual FABP4/5 inhibitors
Anti-lipolytic and anti-inflammatory effects
Metabolic stability
Anti-diabetic activities

ABSTRACT

Fatty acid-binding protein 4 (FABP4) and fatty acid-binding protein 5 (FABP5) are promising therapeutic targets for the treatment of various metabolic diseases. However, the weak potency, low selectivity over FABP3, or poor pharmacokinetic profiles of currently reported dual FABP4/5 inhibitors impeded further research. Here, we described the characterization of a series of dual FABP4/5 inhibitors with improved metabolic stabilities and physicochemical properties based on our previous studies. Among the compounds, **D9** and **E1** exhibited good inhibitory activities against FABP4/5 and favorable selectivity over FABP3 *in vitro*. In cell-based assays, **D9** and **E1** exerted a decrease of FABP4 secretion, a strong anti-lipolytic effect in mature adipocytes, and suppression of MCP-1 expression in THP-1 macrophages. Moreover, **D9** and **E1** possessed good metabolic stabilities in mouse hepatic microsomes and acceptable pharmacokinetics profiles in ICR mice. Further *in vivo* experiments showed that **D9** and **E1** could potently decrease serum FABP4 levels and ameliorate glucose metabolism disorders in obese diabetic *db/db* mice. These results demonstrated that **D9** and **E1** could serve as lead compounds for the development of novel anti-diabetic drugs.

1. Introduction

Type 2 diabetes (T2D) is a chronic metabolic disease characterized by persistent hyperglycemia associated with defects in insulin secretion and insulin action [1], which is considered to be a growing global health problem [2]. The progression of the disease impairs insulin action, disrupts glucose homeostasis and produces hyperglycemia, as well as aggravates insulin resistance of peripheral tissues [3]. Considering the limitations of the current hypoglycemic drugs [4], there is an imperative need for safe and efficient therapeutic agents to develop personalized treatment for T2D patients.

Fatty acid binding protein 4 (FABP4, also known as aP2 or AFABP) is predominantly expressed in adipocytes and macrophages [5], which functions as an intracellular lipid chaperone and is involved in modulating glucose and lipid metabolism and inflammation responses [6]. It has been demonstrated that *Fabp4*-deficient mice acquired modest therapeutic benefits for genetic or dietary obesity-related hyperinsulinemia and insulin resistance [7,8]. Additionally, deletion of *Fabp4* decreased lipolysis both *in vitro* and *in vivo* [9,10] and attenuated the inflammatory response in macrophages [11]. It's worth noting that lack of *Fabp4* in adipocytes led to a compensatory upregulated expression of FABP5, a minor isoform of FABP in adipocytes [12], which might be part of the reason for the modest phenotype of *Fabp4*$^{-/-}$ mice. Similarly, ablation of *Fabp5* enhanced glucose transport in insulin-stimulated adipocytes and increased systemic insulin sensitivity in dietary and genetically obese mice [13]. Compared with *Fabp4* or *Fabp5* single-knockout mice, *Fabp4* and *Fabp5* double-knockout mice (*Fabp4*$^{-/-}$ *Fabp5*$^{-/-}$) exhibited a stronger protection against T2D, non-alcoholic fatty liver disease and atherosclerosis [14,15], indicating that targeting FABP4 and FABP5 simultaneously might be a novel therapeutic approach for the treatment of metabolic diseases. In

* Corresponding author.
** Corresponding author.
*** Corresponding author.
E-mail addresses: liyx417@fudan.edu.cn (Y.-X. Li), hywang@simm.ac.cn (H.-Y. Wang), dingning@fudan.edu.cn (N. Ding).
[1] These authors contributed equally to this work.

https://doi.org/10.1016/j.ejmech.2021.113720
0223-5234/

addition to performing intracellular biological functions, FABP4 can be secreted from adipocytes in associated with lipolysis and act as an adipokine to exert various effects on multiple peripheral tissues, including hepatic glucose production, cardiomyocyte contraction and insulin secretion [16–19]. Elevated serum FABP4 level is closely correlated with the development of a variety of metabolic diseases such as obesity, T2D and cardiovascular diseases [14,20]. Although some agents have been reported to reduce serum concentration of FABP4 [21,22], the modulation of plasma FABP4 level by dual FABP4/5 inhibitors has not been reported.

Some FABP inhibitors have been published over the past decades. Several classes of representative FABP4 and FABP4/5 inhibitors were listed below (Fig. 1). **BMS309403** (**A**) is a specific FABP4 inhibitor that improved glucose homeostasis and insulin sensitivity, reduced adipose tissue inflammation in diabetic mouse models [23]. The 2-(phenylamino) benzoic acid FABP4 inhibitor **B** displayed strong anti-inflammatory activity *in vitro* and *in vivo* [24]. Compounds **C-G** were effective FABP4/5 inhibitors synthesized for the treatment or prophylaxis of T2D, atherosclerosis, chronic kidney diseases, or nonalcoholic steatohepatitis. While these dual FABP4/5 inhibitors were only profiled for inhibitory activity against human FABP4/5 (Ki or IC_{50}), results of the pharmacological evaluation in animal models have not been revealed [25–29]. The dual FABP4/5 inhibitor **H,** featured as a non-carboxylic-acid-containing compound, was reported to show significant potency towards FABP4 and FABP5, and inhibit lipolysis in 3T3-L1 adipocytes and suppress MCP-1 release from THP-1 macrophages as well [30]. However, there is still no FABP inhibitor has entered the clinical research phase in view of some ineligible issues, including poor metabolic properties, toxicities, and potent drug resistances [31]. Therefore, it still needs to make more efforts to bring optimal molecules into therapy.

In our previous study, two novel dual FABP4/5 inhibitors (**A16** and **B22**) were disclosed based on a potent FABP4 inhibitor **16dk** [32]. Unfortunately, the poor hepatic microsomal stability of **A16** and the low dynamic solubility of **B22** hindered further investigations. In this work, to improve the metabolic stability of **A16** and optimize the physicochemical properties of **B22**, two series of novel dual FABP4/5 inhibitors (**D** and **E**, respectively.) basing on these two compounds were designed, synthesized, and comprehensively evaluated *in vitro* and *in vivo*. As the results, compounds **D9** and **E1** were discovered to show high inhibitory activity against FABP4/5, strong anti-lipolytic effect on mature adipocytes, moderate anti-inflammatory effect on THP-1 macrophages, good metabolic stability, acceptable pharmacokinetic profiles, and clear *in vivo* effects.

2. Results and discussion

2.1. Compounds design

Compound **A16** was showed to be good FABP4/FABP5 inhibitor in our previous work (IC_{50} = 1.97 μM for FABP4; IC_{50} = 4.85 μM for FABP5). However, further investigations indicated that **A16** is metabolically labile in mouse liver microsomes (MLM), since the $T_{1/2}$ is only 23.5 min. The preliminary studies on the metabolism products of **A16** in MLM implied that the ether bond (C–O) might be the major potential metabolic site (data not shown). Therefore, the more stable C–C bond was introduced into the molecule to replace the corresponding C–O ether bond (compound **C1**). To our delight, the stability of compound **C1** was greatly improved ($T_{1/2}$ > 500 h in MLM) as compared with that of **A16**. However, the FABP4 inhibitory activity of **C1** was significantly decreased (IC_{50} = 15.65 μM for FABP4; IC_{50} = 3.75 μM for FABP5) in contrast with **A16**. Besides, the lipophilicity of **C1** seems higher than expected (C_{logP} = 7.8). Thus, to improve the FABP4/5 potency and the druggability of **C1**, **Series D** compounds basing on the structure of **C1** were designed, which keeping the C–C bond linker in the side chain between the naphthalene core and the aromatic substitutions (R_1).

As for **B22**, another representative FABP4/5 inhibitor disclosed in our previous work, displayed good potency against FABP4/5 (IC_{50} = 2.63 μM for FABP4; IC_{50} = 8.97 μM for FABP5). However, **B22** showed no lipolytic inhibition in 3T3-L1 adipocytes. Previous work [32,33] indicated that the carboxylic acid is the key for **B22** to keep the FABP4/5 inhibitory activities. Interestingly, a slight modification of **B22** by inserting a CH_2 group between the key carboxylic acid and the phenyl group (**E1**) solved the above problems associated to **B22**. Compound **E1** not only exhibited excellent inhibitions against both FABP4/5 (IC_{50} = 3.78 μM for FABP4; IC_{50} = 5.72 μM for FABP5) but also showed impressive activities on 3T3-L1 adipocytes and THP-1 macrophages. Inspired by this work, series **E** compounds with various R_2 group were designed by keeping the phenylacetic acid group in **B22** to find more potent compounds (Fig. 2).

2.2. Chemistry

The preparation of **D1-12** is depicted in Scheme 1. The synthesis

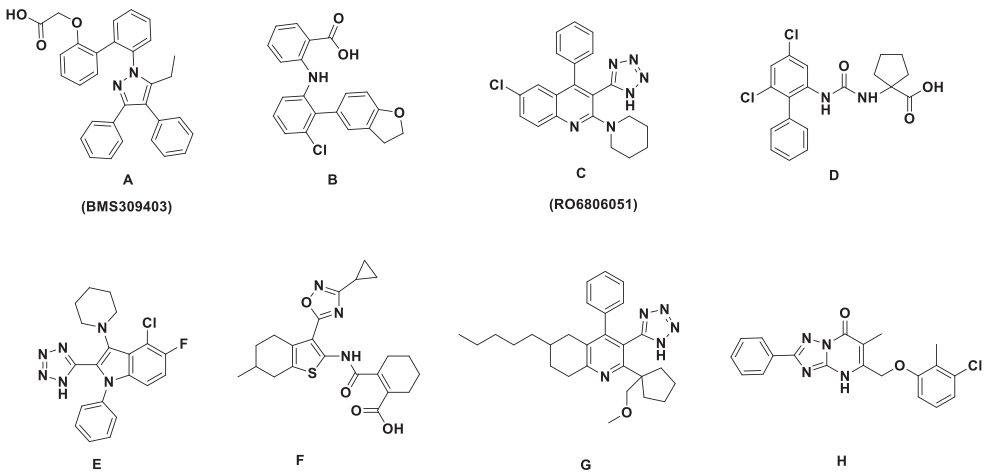

Fig. 1. Representative structures of FABP inhibitors.

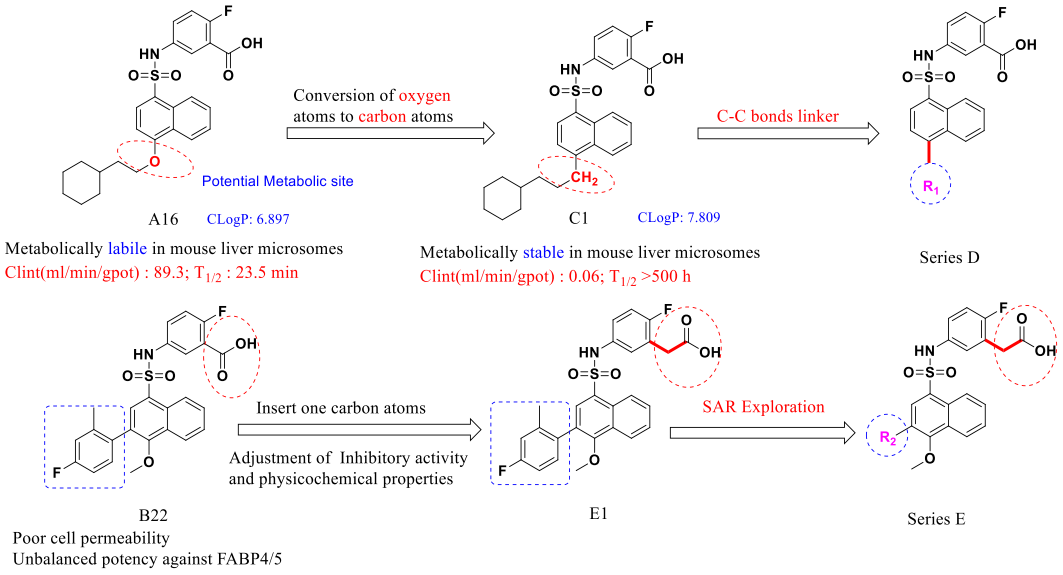

Fig. 2. The Structure optimization strategy based on **A16** and **B22**.

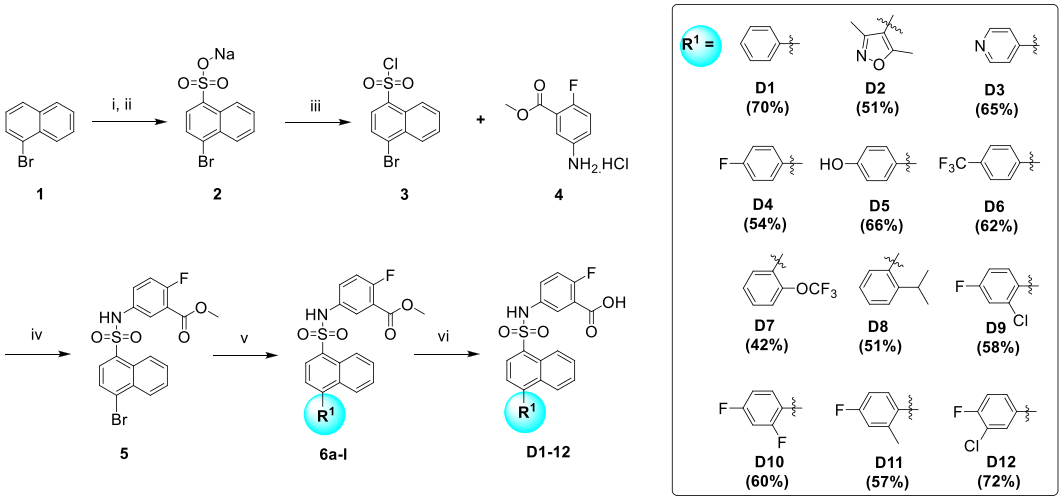

Scheme 1. Synthesis of **D1-12**. Reagents and conditions: (i) HSO_3Cl, $CHCl_3$, 0 °C, 1 h; (ii) NaCl solution; 61 % over 2 steps; (iii) $SOCl_2$, DMF, 0 °C, 1 h, 57 %; (iv) Py, acetone, 55 °C, 1 h, 55 %; (v) $PdCl_2$(dppf), CH_2Cl_2, DMF, K_2CO_3, H_2O, 100 °C, 12 h; (vi) NaOH, H_2O, MeOH, 1 h.

commenced with the commercially available 1-bromonaphthalene (**1**), which was converted to intermediate **2** by treated with chlorosulfonic acid and saturated sodium chloride solution. After transformed to the corresponding sulfonyl chloride by reacted with thionyl chloride in DMF, compound **3** coupled with methyl 5-amino-2-fluorobenzoate hydrochloride (**4**) to yield key intermediate **5**. Then **5** cross-coupled with a panel of aromatic boric acids or borates *via* Suzuki reaction to provide the corresponding products. After hydrolyzing the methyl esters, the designed compounds **D1-12** were prepared.

The preparation of compounds **E1-14** was outlined in Scheme 2, which adopted a similar strategy to that of series **D** (Scheme 2). The commercially available 1-Naphthol (**7**) was converted to the corresponding sulfonyl chloride **10** through three steps [32]. After condensed with phenylamine (**11**), the key intermediate **12** yielded the corresponding cross-coupling products *via* Suzuki reaction. After hydrolyzing the methyl esters, the designed compounds **E1-14** were furnished.

2.3. Biological evaluations

2.3.1. In vitro FABP4 and FABP5 inhibitory activity assays

The inhibitory activities of the compounds against FABP4/5 were evaluated with the 8-anilino-1-naphthalene-sulfonic acid (1, 8-ANS) displacement assay as previously reported [32]. The reported FABP4 inhibitor **BMS309403** and dual FABP4/5 inhibitor compound **H** were used as the positive controls.

The results for **D1-12** are summarized in Table 1. Compared with **A16** (IC_{50}: 1.97 μM for FABP4; IC_{50}: 4.85 μM for FABP5), **D1** displayed a slight decline in FABP4 (IC_{50}: 4.84 μM) and FABP5 potency (IC_{50}: 18.38 μM). These results indicated that replacement of the ether side chain (C—*O*—C) of **A16** to a C—C linked phenyl was well tolerated. Further changing of the phenyl group of **D1** to a 3, 5-dimethylisoxazole or pyridyl group, compounds **D2** and **D3**, respectively, still had moderate inhibition against FABP4 but weak inhibition against FABP5. Since the phenyl-containing compound **D1** seemed better than **D2** and **D3** at the current stage, we carried

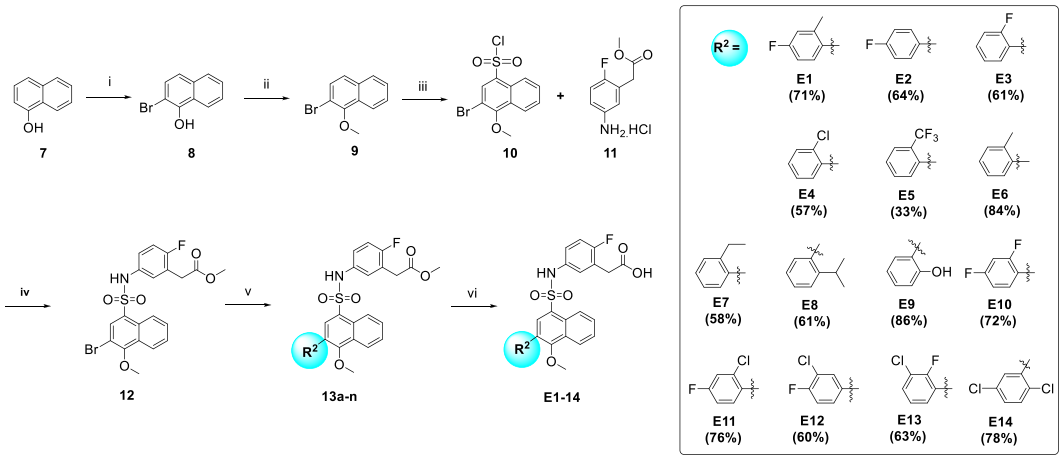

Scheme 2. Synthesis of compounds **E1-E14**. Reagents and conditions: (i) NBS, diethylamine, CH_2Cl_2, 40 °C, overnight, 72 %; (ii) CH_3I, KOH, CH_3CN, 40 °C, 12 h, 85 %; (iii) HSO_3Cl, CH_3Cl, 0 °C to rt.,82 %; (iv) Pyridine, acetone, 55 °C, 1 h, 61 %; (v) R−B(OH)$_2$, K_2CO_3, $PdCl_2$(dppf). CH_2Cl_2, DMF, H_2O; (vi) NaOH, H_2O, MeOH, 1 h, rt.

Table 1
In vitro FABP4 and FABP5 inhibitory activities of **Series D**.

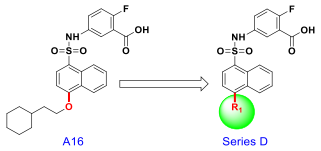

Compound	R^1	FABP4		FABP5	
		@25 μM Inhibition %	IC_{50} (μM)	@25 μM Inhibition %	IC_{50} (μM)
D1		82 %	4.84 ± 0.19	62 %	18.38 ± 0.13
D2		61 %	N.d	19 %	N.d
D3		52 %	N.d	21 %	N.d
D4		80 %	7.68 ± 0.92	59 %	N.d
D5		73 %	8.24 ± 0.13	52 %	N.d
D6		40 %	N.d	64 %	N.d
D7		74 %	12.53 ± 0.71	79 %	8.20 ± 1.03
D8		74 %	11.91 ± 0.31	67 %	16.84 ± 1.90
D9		86 %	4.68 ± 0.13	75 %	10.72 ± 0.33
D10		85 %	4.70 ± 0.19	69 %	14.03 ± 1.03
D11		85 %	5.00 ± 0.19	74 %	11.16 ± 0.33
D12		78 %	7.84 ± 0.17	84 %	6.33 ± 0.83
A16		92 %	1.97 ± 0.15	66 %	4.85 ± 1.03
Compound **H**		97 %	6.34 ± 0.01	52 %	23.42 ± 0.32
BMS309403		99 %	2.36 ± 0.02	N.d	N.d

N.d represent not determined.

out the detailed SAR investigations focusing on the substitutions of the phenyl of **D1**. Introduction of a *para*-substituent on the phenyl group afforded compounds **D4-6**, which all demonstrated decreased potency against FABP4 and comparative inhibitory rates against FABP5. Compounds containing trifluoromethoxy (**D7**) and bulky isopropyl group (**D8**) on the *ortho* position of the phenyl also did not increase the FABP4 inhibition. Introducing halogens or/and methyl to the phenyl group, **D9-12** displayed similar inhibitory activity against FABP4 and improved FABP5 potency to **D1**.

The results for **E1-14** are summarized in Table 2. Optimization of **B22** around the key carboxylic group led to the discovery of **E1**, which showed very good inhibitory activities both on FABP4 (IC_{50}: 3.78 μM) and FABP5 (IC_{50}: 5.72 μM). These results encouraged us to explore the SAR around **E1** deeply. Removing the methyl on the side phenyl of **E1**, compound **E2** kept the inhibitory potency on FABP4 but decreased the FABP5 inhibition around 3 folds. When a single halogen (**E3** or **E4**) or trifluoromethyl (**E5**) was incorporated on the *ortho*-substitutions of the phenyl, there was a decline in FABP4 potency (Inhibition rate: 56 % ~ 87 %). Expanding the substituent from methyl (**E6**) to ethyl (**E7**) and isopropyl (**E8**), the inhibitory potency on FABP4 decreased. It should be noted that compound **E8** bearing 2-isopropyl group was the most potent FABP5 inhibitor that has been reported ever. Incorporation of a hydroxyl group (**E9**) seemed well-tolerated in FABP4 and FABP5 activity. Further modifications on the *ortho*-substitutions of the phenyl group by the introduction of two halogens (**E10-E14**) gave similar inhibitory potency on FABP4 but a slight decreased FABP5 inhibition to **E1**.

The direct binding affinities of **BMS309403**, **D9** and **E1** to FABP4

Table 2
In vitro FABP4 and FABP5 inhibitory activities of **Series E**.

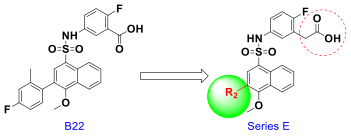

Compound	R^2	FABP4		FABP5	
		@25 μM Inhibition %	IC_{50} (μM)	@25 μM Inhibition %	IC_{50} (μM)
E1		94 %	3.78 ± 0.03	72 %	5.72 ± 0.47
E2		95 %	4.71 ± 0.02	59 %	14.64 ± 1.19
E3		87 %	5.25 ± 0.12	50 %	12.36 ± 0.57
E4		77 %	8.02 ± 0.29	63 %	7.57 ± 0.18
E5		56 %	N.d	63 %	7.72 ± 1.36
E6		80 %	5.16 ± 0.20	62 %	7.72 ± 1.67
E7		63 %	14.28 ± 1.36	74 %	3.20 ± 0.22
E8		50 %	N.d	66 %	2.90 ± 0.18
E9		86 %.	8.03 ± 1.24	55 %	N.d
E10		96 %	3.14 ± 0.05	55 %	10.95 ± 1.67
E11		90 %	4.77 ± 0.11	62 %	6.08 ± 1.21
E12		88 %	5.00 ± 0.40	64 %	12.82 ± 0.99
E13		84 %	6.45 ± 0.07	63 %	11.18 ± 2.81
E14	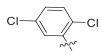	52 %	N.d	60 %	13.33 ± 5.67
B22		95 %	2.63 ± 0.11	67 %	8.97 ± 0.98
Compound **H**		97 %	6.34 ± 0.01	52 %	23.43 ± 0.32
BMS309403		99 %	2.36 ± 0.02	N.d	N.d

N.d represent not determined.

and FABP5 were measured by using microscale thermophoresis (MST). Results showed that the K_d values of **BMS309403**, **D9** and **E1** for FABP4 were 1.67 μM, 11.06 μM and 3.14 μM, respectively (Fig. S3), indicating that **D9** and **E1** showed high affinity to FABP4 as similar as **BMS309403**. The K_d values of **BMS309403**, **D9** and **E1** to FABP5 were 2794.5 μM, 104.9 μM and 14.09 μM, respectively (Fig. S4), which suggested **E1** has a strong binding affinity to FABP5.

2.3.2. FABP3 selectivity evaluation

It is worth noting that *Fabp3*-deficient mice suffered from reduced tolerance to physical activity and regional cardiac hypertrophy [34]. Considering the potential cardiotoxicity caused by FABP3 inhibition, it is of significant importance to consider the FABP3 selectivity while developing dual FABP4/5 inhibitors. Basing on the above screening, dual FABP4/5 inhibitors (**D9**, **D12**, **E1**) were evaluated for their selectivity against FABP3/4/5 (Table 3). **BMS309403** and compound **H** were used as the positive controls. The results showed all the selected compounds had much lower inhibitory activities than those of the controls. Besides, the selectivities of these compounds against FABP4 and FABP5 over FABP3 are excellent as compared with those of the controls.

2.3.3. Effects of dual FABP4/5 inhibitors on lipolysis in mature adipocytes

Pharmacological inhibition or deletion of FABP4 in adipocytes exhibited reduced efficiency of lipolysis [35,36]. Therefore, we selected several potent dual FABP4/5 inhibitors from series D (**D9**, **D10**, **D11**, **D12**) and series E (**E1**, **E4**, **E8**, **E11**) to investigate their anti-lipolytic effects on Forskolin (FSK)-stimulated mature adipocytes, with the FABP4 inhibitor **BMS309403** and dual FABP4/5 inhibitor **B22** as the positive controls. Firstly, the Cell Counting Kit (CCK-8) assay was carried out to examine the cytotoxicity effects of the selected compounds on 3T3-L1 preadipocytes at the concentration of 100 μM. As shown in Fig. S1, all of the compounds had no significant effects on the cell viability of adipocytes. The lipolysis experiment was then performed at the concentration of 80 μM, and the result was demonstrated in Fig. 3A and B. FSK significantly increased the concentration of glycerol released from mature adipocytes, and our compounds as well as **BMS309403** robustly inhibited the FSK-stimulated lipolysis in 3T3-L1 cells, while **B22** exhibited no anti-lipolytic effect, validating the feasibility of series **E** design strategy. Among the compounds, **D9**, **D11**, **E4** showed comparative potency with that of **BMS309403**, while **E1** and **E8** showed superior anti-lipolytic activity than that of **BMS309403.**

2.3.4. In vitro liver microsomal stability

Based on the potency at the molecular- and cellular-level screenings described above, dual FABP4/5 inhibitors **D9**, **D11**, **E1**, **E4** and **E8** were subjected to evaluate the *in vitro* metabolic stability in MLM. The results were summarized in Table 4. As compared with **A16**, compounds **D9** and **D11** exhibited improved metabolic stability in MLM, reflected in the remarkable increase in the half-time and a sharp decline in clearance ratio. In contrast with **B22**, compound **E1** exhibited a slight decrease of liver microsomal stability within the acceptable range. Besides, compound **E4** and **E8**, which displayed strong anti-lipolytic activities in mature adipocytes, exhibited poor metabolic stability in MLM. Considering the above results, **D9** and **E1** were selected to futher explore the anti-inflammatory effects on THP-1 macrophages.

2.3.5. Anti-inflammatory effects of dual FABP4/5 inhibitors on THP-1 macrophages

FABP4 deficiency in macrophages could suppress inflammatory signaling responses by decreasing the production of pro-inflammatory cytokines such as MCP-1/CCL2 [37]. It had also been demonstrated that **BMS309403** reduced the release of MCP-1 from THP-1 macrophages in a FABP4-dependent manner [23]. In our study, based on the results of anti-lipolytic activity and liver microsomal stability described above, **D9** and **E1** were selected to investigate the anti-inflammatory effects on THP-1 macrophages, **BMS309403** was chosen as positive control. Firstly, the cytotoxicity was detected by the CCK-8 assay, and the results showed that all the compounds had no effects on the cell viability of THP-1 cells at the concentration of 50 μM (Fig. 4A). The expression of pro-inflammatory cytokines MCP-1 were robustly increased after the stimulation of LPS, and compound **D9**, **E1** and **BMS309403** dramatically decreased the expression of MCP-1 in LPS-stimulated THP-1 macrophages (Fig. 4B). The data suggested that dual FABP4/5 inhibitors may exert anti-inflammatory effect by inhibiting the expression of MCP-1 in macrophages.

2.4. In vivo pharmacokinetic properties

Pharmacokinetic studies of **D9**, **E1** and **BMS309403** was conducted in ICR (CD1) mice at 1 mg/kg and 3 mg/kg doses for intravenous (iv) and oral (po) administration, respectively. As shown in Table 5, compared with the FABP4 inhibitor **BMS309403**, **D9** and **E1** possessed more favorable PK profiles with a relative longer half-life ($T_{1/2}$ (po^a): **D9** = 1.36 h; **E1** = 6.04 h *vs.* **BMS309403** = 0.63 h), higher system exposure (AUC (po^a): **D9** = 1093 (h*ng/mL); **E1** = 1742 (h*ng/mL) *vs.* **BMS309403** = 90 (h*ng/mL)), lower plasma clearance level (CL: **D9** = 8.73 (mL/min/kg); **E1** = 8.56 (mL/min/kg) *vs.* **BMS309403** = 44.3 (mL/min/kg)) and better oral bioavailability (F: 18.4 % for **D9** and 29.9 for **E1** *vs.* 7 % for **BMS309403**). All these results indicated that **D1** and **E1** were suitable for *in vivo* efficacy evaluation.

*2.5. In vivo anti-diabetic efficacy of **D9** and **E1***

To gain insight into the potential therapeutic effects of **D9** and **E1** *in vivo*, the studies in obese diabetic *db/db* mice were carried out. The FABP4 inhibitor **BMS309403** was used as the positive control. Six-week-old C57BL/KsJ-db/db mice were orally administrated with **D9**, **E1** and **BMS309403** at a dose of 50 mg/kg for 8 weeks. First, all the three compounds **D9**, **E1** and **BMS309403** had no obvious effects on body weight (Fig. S2A). As showed in Fig. 5A, D9 and E1 reduced the fasting blood glucose levels by 32.4 % and 28.1 % at the 7th week as compared with that of the vehicle group, while

Table 3
Selectivity of representative FABP4/5 inhibitor toward FABP3.

Compound	FABP3 IC_{50} (μM)	FABP4 IC_{50} (μM)	FABP5 IC_{50} (μM)	FABP3/FABP4	FABP3/FABP5
D9	103.70 ± 3.54	4.68 ± 0.13	10.72 ± 0.33	22.15	9.67
D12	103.05 ± 0.49	7.84 ± 0.17	6.33 ± 0.83	13.14	16.27
E1	84.36 ± 1.91	3.78 ± 0.03	5.72 ± 0.47	22.31	14.74
BMS309403	35.78 ± 2.12	2.36 ± 0.02	N.d	15.16	N.d
Compound **H**	1.95 ± 0.01	6.34 ± 0.01	23.42 ± 0.32	0.31	0.08

N.d represent not determined.

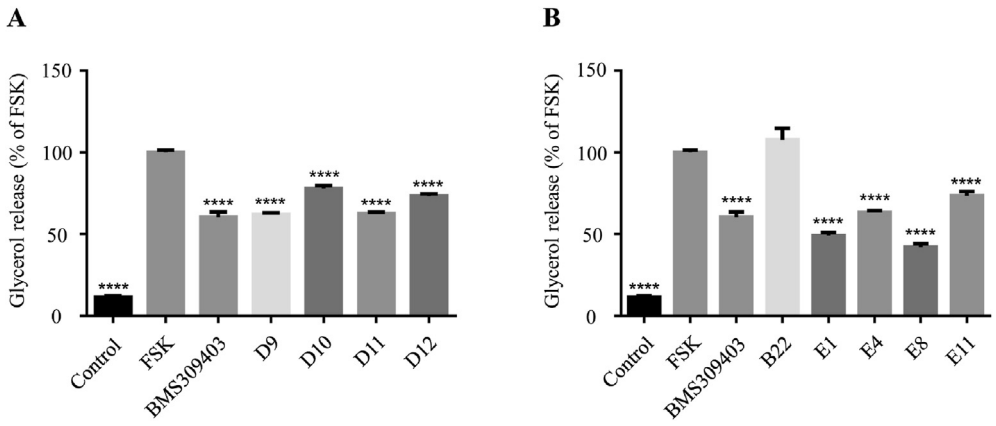

Fig. 3. (A) Effect of representative Series D compounds and **BMS309403** on the release of glycerol from FSK-stimulated mature adipocytes at the concentration of 80 μM. (B) Effect of representative Series E compounds, **BMS309403** and **B22** on the release of glycerol from FSK-stimulated mature adipocytes at the concentration of 80 μM (n = 6/group). $^{**}p < 0.01$, $^{****}p < 0.0001$vs. FSK group.

Table 4
Mouse liver microsomal stability of representative compounds.

Compd.	$T_{1/2}$ (min)	*Clint* (ml/min/gpot)
A16	23.5	89.3
D9	91	23.1
D11	88.4	23.8
B22	102.1	20.6
E1	88.3	23.8
E4	43.1	48.8
E8	15.1	139.1

Table 5
In Vivo PK parameters for **D9**, **E1**, and **BMS309403** in mice.

Parameter	D9	E1	BMS309403
$T_{1/2}$ (po[a]) (h)	1.36 ± 0.13	6.04 ± 7.37	0.63 ± 0.23
$T_{1/2}$ (iv[a]) (h)	2.88 ± 2.16	1.78 ± 0.10	1.53 ± 0.17
Cmax (ng/mL)	782 ± 463	478 ± 195	151 ± 58
AUC (po) (h*ng/mL)	1093 ± 21	1742 ± 516	90 ± 29
AUC (iv) (h*ng/mL)	1981 ± 484	1941 ± 383	427 ± 185
Cl (mL/min/kg)	8.73 ± 2.52	8.56 ± 1.69	44.3 ± 20.1
F (%)	18.4	29.9	7

[a] po (3 mg/kg); iv (1 mg/kg). Results are expressed as the mean ± SEM (n = 3).

BMS309403 treatment exhibited the better reducing levels by 38.9 % at the same dose. Subsequently, the results of OGTT (Fig. 5B and C) and ITT (Fig. 5D and E) along with Western blot of liver (Fig. 5F and G) revealed a significant improvement of glucose metabolism and insulin resistance in *db/db* mice treated with **D9** and **E1**. In addition, **D9**, **E1** and **BMS309403** treatment significantly elevated the serum level of high-density cholesterol (HDL-C) (Fig. 5H), and compound **D9** significantly reduced serum low-density lipoprotein cholesterol (LDL-C) level (Fig. 5I). However, the selected compounds had no effects on the serum level of triglyceride (TG) and total cholesterol (TCH) (Figs. S2B–C). Further investigations showed that the serum FABP4 level was dramatically decreased by **D9** and **E1** (Fig. 5J). It had been reported that FABP4 was secreted from adipocytes and elevated circulating FABP4 was associated with various metabolic diseases [14,38]. Reduced circulating FABP4 levels was associated with improved metabolic benefits [39].

We subsequently examined the effects of **D9** and **E1** on the release of FABP4 from mature adipocytes. As shown in Fig. 6A–C, compared with the control group, the FABP4 levels in the supernatant were dramatically reduced by **D9** and **E1** at the concentration of 50 μM, which might explain the reduction of circulating FABP4 levels.

Overall, the above investigations revealed that **D9** and **E1** acted as effectively as **BMS309403** on reducing the fasting blood glucose

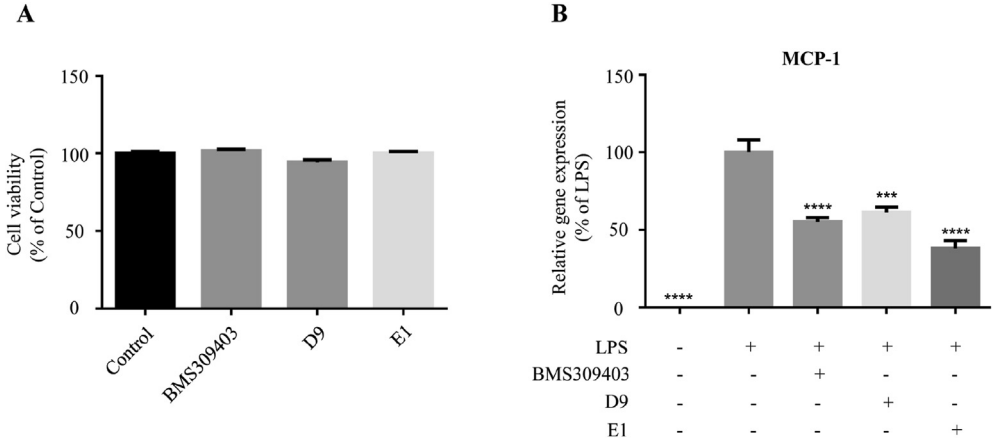

Fig. 4. (A) Effects of compounds on the viability of THP-1 macrophages. Cell viability was determined by CCK-8 assay (n = 6/group). (B) Effects of compounds on the gene expression of MCP-1 in LPS-stimulated THP-1 macrophages. Gene expression level of cytokines was measured by RT-qPCR (n = 4/group). $^{***}p < 0.001$, $^{****}p < 0.0001$ vs. LPS group.

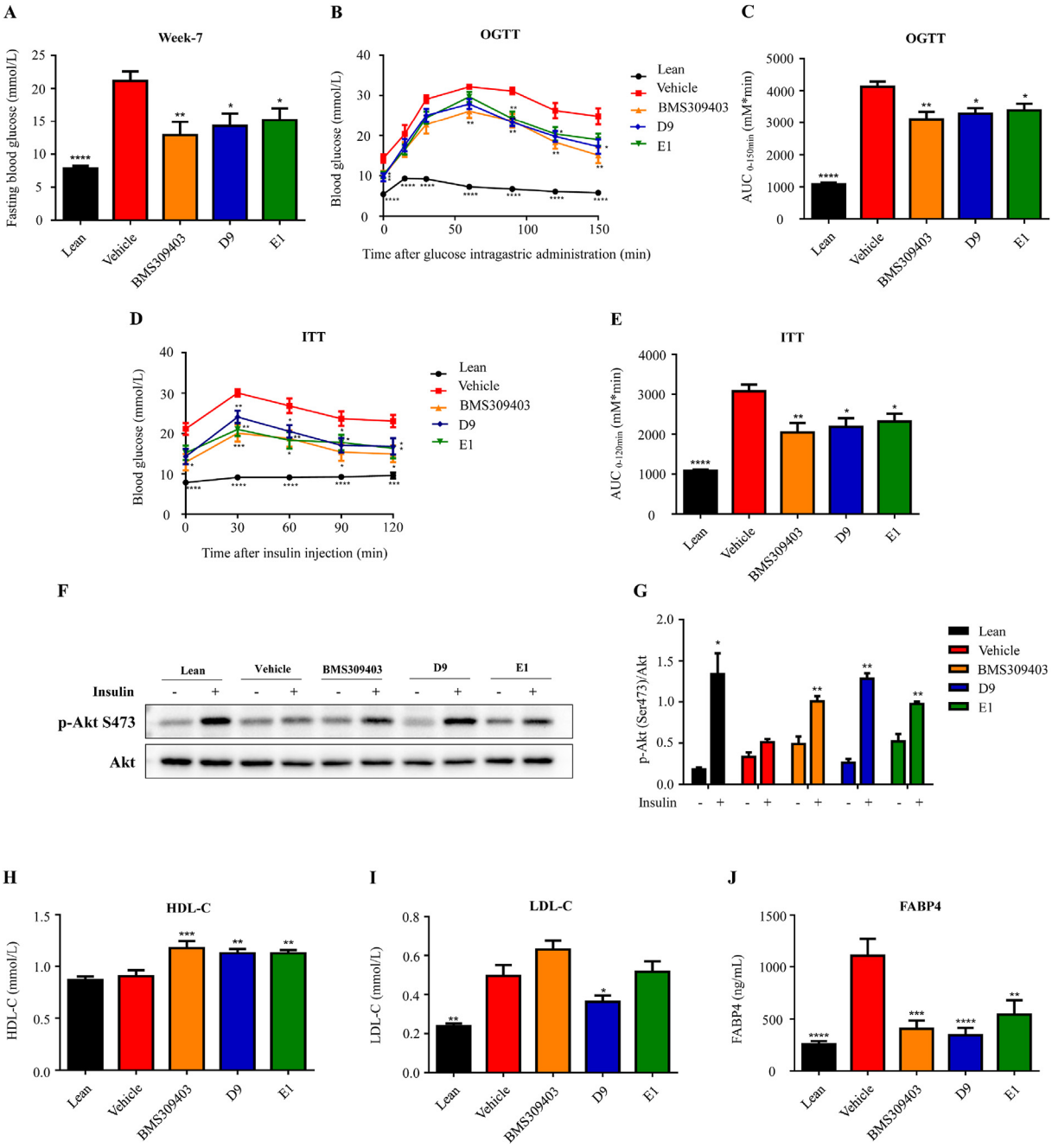

Fig. 5. Effects of **D9**, **E1** and **BMS309403** on glucose and lipid metabolism in *db/db* mice. (A) Six-hour fasting blood glucose level after 7-weeks of administration. (B–C) After 45-days of administration, the mice were subjected to oral glucose tolerance test (OGTT). (D–E) After 51-days of administration, mice were subjected to insulin tolerance test (ITT). Blood glucose level of indicated time points were measured and the AUC was calculated. (F–G) Representative blots of hepatic Akt and *p*-Akt (Ser473) and the statistical results of bands analysis data. (H–J) Serum HDL-C, LDL-C and FABP4 level of mice in the vehicle, compound-treated and lean groups. All serum parameters were measured using assay kits. $^{*}p < 0.05$, $^{**}p < 0.01$, $^{***}p < 0.001$, $^{****}p < 0.0001$ vs. vehicle group. Values are given as mean ± S.E.M (n = 10/group).

levels, improving the oral glucose tolerance and insulin resistance in the obese diabetic db/db mice, and exerted a certain degree of amelioration on lipid metabolism disorders. It should be noted that **BMS309403** is not a neat FABP4 inhibitor and it could also activate AMPK signaling pathway and thus promotes glucose uptake in skeletal muscle cells [40]. The inhibition of FABP4 and simultaneous activation of AMPK signaling pathway made **BMS309403** play strong effects on the anti-diabetic tests. On the other hand, our compounds are potent dual FABP4/5 inhibitors. As mentioned above, inhibition of Fabp4 in adipocytes led to the compensatory upregulated expression of FABP5 in adipocytes [12]. FABP5 could also cause the problems on glucose and lipid metabolism as FABP4 did [12]. Simultaneously targeting FABP4 and FABP5 should be a novel therapeutic approach for the treatment of metabolic diseases. Thus, our potent dual FABP4/5 inhibitors **D9** and **E1** could still be regarded as useful lead compounds for personalized antidiabetic treatment, even if they did not show strong advantages on glucose and lipid metabolism in *db/db* mice as compared with **BMS309403** from the data of Fig. 5.

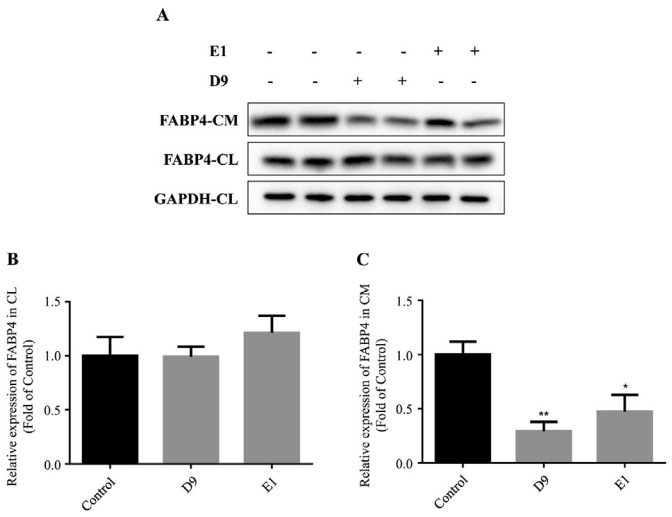

Fig. 6. (A) Immunoblots of FABP4 and glyceraldehyde 3-phosphate dehydrogenase (GAPDH) using the cell lysate (CL) and conditioned medium (CM) for 24 h of mature adipocytes at the concentration of 50 μM. (B–C) Densitometric analysis of the immunoblots of FABP4 in CL and CM. Data are expressed as mean ± S.E.M and are representative of three independent experiments. *$p < 0.05$, **$p < 0.01$ vs. Control group.

3. Conclusion

In summary, we have prepared a series of potent and selective dual FABP4/5 inhibitors with potential therapeutic effects in diabetic mouse model based on our previous study. Systematic SAR explorations resulted in the identification of **D9** and **E1** with favorable FABP4/FABP5 inhibitory activity for further investigation. Compound **D9** and **E1** could not only potently inhibit the lipolysis in FSK-stimulated mature adipocytes as well as the release of FABP4, but also decreased the expression of MCP-1 in LPS-stimulated THP-1 macrophages. Furthermore, compounds **D9** and **E1** showed good metabolic stability in mouse liver microsomes and decent PK properties in mice, and long-term oral administration of **D9** and **E1** at the dose of 50 mg/kg could effectively ameliorate glucose metabolic disorders in obese diabetic *db/db* mice. Additionally, the serum FABP4 level was prominent decreased by **D9** and **E1**. These data indicated that **D9** and **E1** could be regarded as useful lead compounds to be developed into personalized oral antidiabetic agents with acceptable efficacy and safety.

4. Experiment section

4.1. General information

All the reagents and solvents were supplied by standard suppliers without further purification. Reactions were monitored by analytical thin layer chromatography (TLC) and visualized with a UV lamp (254 nm). The column chromatography was carried out using silica gel (200–300 mesh). ^{1}H NMR and ^{13}C NMR spectra were recorded with a 400 MHz Varian or Bruker 600 MHz NMR spectrometer at ambient temperature, respectively. Coupling constants (J) values are described as hertz and Chemical shifts (δ) of NMR spectra are expressed in parts per million (ppm) units downfield from tetramethylsilane. Mass spectra (MS) of compounds were measured on Agilent 6120 quadrupole LC/MS. High resolution mass spectrometry (HRMS) determinations for all new compounds were performed on AB SCIWX TRIPLETOF 5600+.

4.2. General method of synthesizing series D and series E

4.2.1. Preparation of intermediate ***2***

To a solution of 1-bromonaphthalene (2.0 g, 9.66 mmol) in chloroform (15 ml) was added chlorosulfonic acid (1.69 g, 14.49 mmol) dropwise in ice bath. Then the mixture was moved to room temperature and stirred for another 1 h. The mixture was poured into cold water, extracted with ethyl acetate. Next, saturated sodium chloride solution was added to the above ethyl acetate solution under stirring conditions and a white solid was precipitated, the suspension was filtered, and the residue was washed with dichloromethane. The washed residue was dried to obtain the desired derivatives of sodium 4-bromonaphthalene-1-sulfonate as white solid (1.8 g, 61 %).

4.2.2. Preparation of intermediate ***3***

To a solution of intermediate 2 (1.5 g, 4.85 mmol) in DMF (8 mL) was added thionyl chloride (2.89 g, 24.26 mmol) at 0 °C and then stirred at room temperature for another 1 h. The reaction system was poured into the ice water, extracted with extracted with ethyl acetate three times. The combined ethyl acetate layer was sequentially washed with water, dried with anhydrous Na_2SO_4, and concentrated to give the desired product as a brown oil (0.87 g, 57 %), which was used for the next step without further purification.

4.2.3. Preparation of intermediate ***5***

To a solution of intermediate 3 (800 mg, 2.62 mmol) in acetone (10 mL) was added methyl 5-amino-2-fluorobenzoate hydrochloride (538 mg, 2.62 mmol) and pyridine (0.63 ml, 7.85 mmol). The mixture then was refluxed for 2 h and evaporated under vacuum. The residue was diluted with water and extracted with ethyl acetate (15 mL) three times. The combined ethyl acetate layer was sequentially washed with brine, dried with anhydrous Na_2SO_4, and concentrated to give the crude product. The crude was purified by column chromatography with petroleum/ethyl acetate to yield intermediate **4** as a prey solid (0.63 g, 54.9 %).

4.2.4. General procedure for the preparation of intermediates ***6a-l***

To a suspension of the intermediate **5** (1 equiv) in DMF (8 mL) was sequentially added appropriate substituted aryl boric acid (1.3 equiv), K_2CO_3 (2 equiv), $PdCl_2$ (dppf).CH_2Cl_2 (0.1 equiv) and water (0.5 mL). After refluxing for 12 h under N_2 atmosphere, the reaction mixture was cooled and then poured into H_2O. The mixture was extracted with extracted with EtOAc (2x), washed with saturated NaCl solution, dried over anhydrous Na_2SO_4, and concentrated in vacuo. The residue was purified by silica gel column chromatography to afford the target compounds as a white solid.

4.2.5. General procedure for the preparation of ***D1–12***

To a solution of intermediate 6a-6l (1 equiv) in methanol (8 mL) was added 1 N NaOH solution (10 equiv) and stirred at room temperature for 1 h. Then the solvent was removed under vacuum, the residue was acidified to pH = 2 with HCl (1 M) solution and white solid precipitated. The mixture was extracted with ethyl acetate twice and the combined organic layer was dried over anhydrous sodium sulfate and concentrated to provide the target compounds as white solid.

*4.2.5.1. 2-Fluoro-5-((4-phenylnaphthalene)-1-sulfonamido) benzoic acid (**D1**).* White solid, yield: 70 %. ^{1}H NMR (400 MHz, DMSO-d_6) δ 13.34 (s, 1H), 10.96 (s, 1H), 8.78 (d, J = 8.6 Hz, 1H), 8.23 (d, J = 7.5 Hz, 1H), 7.87 (d, J = 8.5 Hz, 1H), 7.78 (t, J = 7.7 Hz, 1H), 7.65 (t, J = 7.7 Hz, 1H), 7.55–7.51 (m, 5H), 7.48–7.43 (m, 2H), 7.32–7.28 (m, 1H), 7.18 (t, J = 9.6 Hz, 1H). ^{13}C NMR (150 MHz, DMSO-d_6) δ 164.20,

156.54, 145.69, 138.53, 133.52, 133.33, 131.59, 129.46, 129.17, 128.42, 128.07, 127.90, 127.80, 127.20, 126.60, 125.24, 124.44, 122.26, 119.53, 117.84. ESI-HRMS [M − H]$^-$ calcd for $C_{23}H_{16}FNO_4S$: 420.0711, found: 420.0713.

*4.2.5.2. 5-((4-(3,5-dimethylisoxazol-4-yl)naphthalene)-1-sulfonamido)-2-fluorobenzoic acid (**D2**).* White solid, yield: 51 %. ^{1}H NMR (400 MHz, DMSO-d_6) δ 10.92 (s, 1H), 8.79 (dd, J = 8.8, 3.1 Hz, 1H), 8.19 (dd, J = 7.6, 3.1 Hz, 1H), 7.83−7.78 (m, 1H), 7.73−7.65 (m, 2H), 7.58 (dd, J = 7.7, 3.1 Hz, 1H), 7.44−7.41 (m, 1H), 7.30−7.27 (m, 1H), 7.22−7.13 (m, 1H), 2.20 (s, 3H), 1.97 (s, 3H). ^{13}C NMR (150 MHz, DMSO-d_6) δ 166.49, 164.13, 158.64, 158.43, 134.34, 133.56, 133.34, 132.09, 129.02, 128.22, 127.71, 126.95, 126.11, 126.05, 124.71, 122.93, 119.49, 117.79, 113.42, 11.07, 9.94. ESI-HRMS [M − H]$^-$ calcd for $C_{22}H_{17}FN_2O_5S$: 439.0769, found: 439.0773.

*4.2.5.3. 2-Fluoro-5-((4-(pyridin-4-yl)naphthalene)-1-sulfonamido) benzoic acid (**D3**).* White solid, yield: 65 %. ^{1}H NMR (400 MHz, DMSO-d_6) δ 11.03 (s, 1H), 8.81 (d, J = 8.8 Hz, 1H), 8.75−8.72 (m, 2H), 8.26 (d, J = 7.6 Hz, 1H), 7.83−7.80 (m, 2H), 7.71−7.64 (m, 1H), 7.59 (d, J = 7.5 Hz, 1H), 7.58−7.48 (m, 3H), 7.34−7.28 (m, 1H), 7.18 (t, J = 9.6 Hz, 1H). ^{13}C NMR (150 MHz, DMSO-d_6) δ 164.20, 158.27, 156.59, 149.68, 146.20, 142.83, 134.43, 133.41, 130.92, 129.02, 128.18, 127.69, 126.11, 125.35, 125.31, 124.58, 124.43, 122.35, 119.61, 117.87. ESI-HRMS [M − H]$^-$ calcd for $C_{22}H_{15}FN_2O_4S$: 421.0664, found: 421.0665.

*4.2.5.4. 2-Fluoro-5-((4-(4-fluorophenyl)naphthalene)-1-sulfonamido)benzoic acid (**D4**).* White solid, yield: 54 %. ^{1}H NMR (400 MHz, DMSO-d_6) δ 10.99 (s, 1H), 8.79 (d, J = 8.7 Hz, 1H), 8.23 (d, J = 7.6 Hz, 1H), 7.84 (d, J = 8.5 Hz, 1H), 7.79 (t, J = 7.7 Hz, 1H), 7.65 (t, J = 7.7 Hz, 1H), 7.55−7.49 (m, 4H), 7.37 (t, J = 8.6 Hz, 2H), 7.34−7.27 (m, 1H), 7.17 (t, J = 9.6 Hz, 1H). ^{13}C NMR (150 MHz, DMSO-d_6) δ 164.20, 162.74, 156.54, 144.57, 134.82, 133.51, 131.63, 131.57, 129.11, 127.94, 127.78, 127.30, 126.48, 125.41, 125.25, 124.47, 122.26, 119.57, 117.83, 115.42. ESI-HRMS [M − H]$^-$ calcd for $C_{23}H_{15}F_2NO_4S$: 438.0617, found: 438.0621.

*4.2.5.5. 2-Fluoro-5-((4-(4-hydroxyphenyl)naphthalene)-1-sulfonamido)benzoic acid(**D5**).* White solid, yield: 66 %. ^{1}H NMR (400 MHz, DMSO-d_6) δ 10.93 (s, 1H), 9.79 (s, 1H), 8.76 (d, J = 8.6 Hz, 1H), 8.20 (d, J = 7.6 Hz, 1H), 7.96 (d, J = 8.5 Hz, 1H), 7.76 (t, J = 7.7 Hz, 1H), 7.63 (t, J = 7.7 Hz, 1H), 7.54−7.52 (m, 1H), 7.48 (d, J = 7.6 Hz, 1H), 7.28 (d, J = 7.9 Hz, 3H), 7.16 (t, J = 9.6 Hz, 1H), 6.92 (d, J = 8.1 Hz, 2H). ^{13}C NMR (150 MHz, DMSO-d_6) δ 164.21, 158.17, 157.45, 145.96, 133.57, 132.54, 131.74, 130.79, 129.29, 129.00, 127.91, 127.76, 126.93, 126.81, 125.15, 124.98, 124.37, 122.17, 119.55, 117.80, 115.27. ESI-HRMS [M − H]$^-$ calcd for $C_{23}H_{16}FNO_5S$: 436.0660, found: 436.0664.

*4.2.5.6. 2-Fluoro-5-((4-(4-(trifluoromethyl)phenyl)naphthalene)-1-sulfonamido)benzoic acid (**D6**).* White solid, yield: 62 %. ^{1}H NMR (400 MHz, DMSO-d_6) δ 11.01 (s, 1H), 8.81 (d, J = 8.6 Hz, 1H), 8.26 (d, J = 7.6 Hz, 1H), 7.90 (d, J = 7.8 Hz, 2H), 7.81 (t, J = 7.2 Hz, 2H), 7.71−7.64 (dd, J = 18.1, 8.0 Hz, 3H), 7.60 (d, J = 7.6 Hz, 1H), 7.56−7.53 (m, 1H), 7.32−7.29 (m, 1H), 7.18 (t, J = 9.6 Hz, 1H). ^{13}C NMR (151 MHz, DMSO-d_6) δ 164.19, 158.26, 156.57, 144.01, 142.71, 134.11, 133.45, 131.31, 130.43, 129.03, 128.09, 127.73, 127.55, 126.31, 125.47, 125.30, 124.54, 122.32, 119.57, 117.70. ESI-HRMS [M − H]$^-$ calcd for $C_{24}H_{15}F_4NO_4S$: 488.0589, found: 488.0589.

*4.2.5.7. 2-Fluoro-5-((4-(2-(trifluoromethoxy)phenyl)naphthalene)-1-sulfonamido)benzoic acid (**D7**).* White solid, yield: 42 %. ^{1}H NMR (400 MHz, DMSO-d_6) δ 13.28 (s, 1H), 10.92 (s, 1H), 8.79 (d, J = 8.7 Hz, 1H), 8.21 (d, J = 7.6 Hz, 1H), 7.77 (t, J = 7.8 Hz, 1H), 7.68−7.60 (m, 2H), 7.57−7.46 (m, 6H), 7.25−7.21 (m, 1H), 7.11 (t, J = 9.7 Hz, 1H). ^{13}C NMR (150 MHz, DMSO-d_6) δ 164.09, 156.71, 145.64, 140.07, 133.96, 133.29, 132.04, 131.80, 130.49, 128.97, 128.01, 127.62, 127.37, 127.33, 126.17, 125.97, 125.65, 125.59, 124.39, 122.70, 121.14, 120.35, 119.44, 117.65. ESI-HRMS [M − H]$^-$ calcd for $C_{24}H_{15}F_4NO_5S$: 504.0534, found: 504.0538.

*4.2.5.8. 2-Fluoro-5-((4-(2-isopropylphenyl)naphthalene)-1-sulfonamido)benzoic acid (**D8**).* White solid, yield: 51 %. ^{1}H NMR (400 MHz, DMSO-d_6) δ 13.16 (s, 1H), 10.85 (s, 1H), 8.77 (d, J = 8.7 Hz, 1H), 8.16 (d, J = 7.5 Hz, 1H), 7.75 (t, J = 7.8 Hz, 1H), 7.57 (t, J = 7.9 Hz, 1H), 7.51−7.37 (m, 5H), 7.31−7.23 (m, 2H), 7.15 (d, J = 9.9 Hz, 1H), 7.09 (d, J = 7.8 Hz, 1H), 2.18−2.12 (m, 1H), 0.92 (dd, J = 6.6, 3.1 Hz, 6H). ^{13}C NMR (150 MHz, DMSO-d_6) δ 164.08, 158.42, 146.38, 145.38, 136.91, 133.41, 133.01, 132.55, 129.18, 128.60, 127.96, 127.35, 127.10, 126.60, 126.01, 125.47, 125.34, 125.16, 124.39, 122.89, 119.36, 117.52, 29.67, 24.07, 22.69. ESI-HRMS [M − H]$^-$ calcd for $C_{26}H_{22}FNO_4S$: 462.1181, found: 462.1187.

*4.2.5.9. 5-((4-(2-chloro-4-fluorophenyl)naphthalene)-1-sulfonamido)-2-fluorobenzoic acid (**D9**).* White solid, yield: 58 %. ^{1}H NMR (400 MHz, DMSO-d_6) δ 11.01 (s, 1H), 8.81 (d, J = 8.6 Hz, 1H), 8.26 (d, J = 7.6 Hz, 1H), 7.90 (d, J = 7.8 Hz, 2H), 7.81 (t, J = 7.2 Hz, 2H), 7.71−7.64 (dd, J = 18.1, 8.0 Hz, 3H), 7.60 (d, J = 7.6 Hz, 1H), 7.56−7.53 (m, 1H), 7.32−7.29 (m, 1H), 7.18 (t, J = 9.6 Hz, 1H). ^{13}C NMR (151 MHz, DMSO-d_6) δ 164.19, 158.26, 156.57, 144.01, 142.71, 134.11, 133.45, 131.31, 130.43, 129.03, 128.09, 127.73, 127.55, 126.31, 125.47, 125.30, 124.54, 122.32, 119.57, 117.70. ESI-HRMS [M − H]$^-$ calcd for $C_{23}H_{14}ClF_2NO_4S$: 472.0227, found: 472.0228.

*4.2.5.10. 5-((4-(2,4-difluorophenyl)naphthalene)-1-sulfonamido)-2-fluorobenzoic acid (**D10**).* White solid, yield: 60 %. ^{1}H NMR (400 MHz, DMSO-d_6) δ 11.02 (s, 1H), 8.80−8.77 (m, 1H), 8.26−8.23 (m, 1H), 7.82−7.77 (m, 1H), 7.69−7.58 (m, 3H), 7.57−7.44 (m, 3H), 7.33−7.26 (m, 2H), 7.21−7.15 (m, 1H). ^{13}C NMR (150 MHz, DMSO-d_6) δ 164.19, 161.63, 158.27, 156.58, 138.57, 134.47, 133.44, 132.92, 131.86, 128.93, 128.12, 127.56, 127.46, 126.38, 126.22, 125.29, 125.23, 124.50, 122.32, 119.60, 117.85, 112.00, 104.21. ESI-HRMS [M − H]$^-$ calcd for $C_{23}H_{14}F_3NO_4S$: 456.0523, found: 456.0525.

*4.2.5.11. 2-Fluoro-5-((4-(4-fluoro-2-methylphenyl)naphthalene)-1-sulfonamido)benzoic acid (**D11**).* White solid, yield: 57 %. ^{1}H NMR (400 MHz, DMSO-d_6) δ 13.23 (s, 1H), 10.89 (s, 1H), 8.78 (d, J = 8.3 Hz, 1H), 8.19 (d, J = 7.4 Hz, 1H), 7.77 (t, J = 7.7 Hz, 1H), 7.61 (t, J = 7.6 Hz, 1H), 7.49−7.39 (m, 3H), 7.32−7.20 (m, 3H), 7.17−7.13 (m, 2H), 1.83 (s, 3H). ^{13}C NMR (150 MHz, DMSO-d_6) δ 164.12, 162.54, 156.68, 144.29, 138.51, 134.44, 133.48, 133.40, 132.05, 131.26, 129.19, 127.97, 127.50, 127.37, 126.28, 125.93, 125.38, 124.52, 122.82, 119.48, 117.59, 116.52, 112.61, 19.28. ESI-HRMS [M − H]$^-$ calcd for $C_{24}H_{17}F_2NO_4S$: 452.0774, found: 452.0777.

*4.2.5.12. 5-((4-(3-chloro-4-fluorophenyl)naphthalene)-1-sulfonamido)-2-fluorobenzoic acid (**D12**).* White solid, yield: 72 %. ^{1}H NMR (400 MHz, DMSO-d_6) δ 11.01 (s, 1H), 8.79 (d, J = 8.6 Hz, 1H), 8.23 (d, J = 7.6 Hz, 1H), 7.86−7.77 (m, 2H), 7.73 (d, J = 7.1 Hz, 1H), 7.67 (t, J = 7.7 Hz, 1H), 7.61−7.52 (m, 3H), 7.50−7.48 (m, 1H), 7.32−7.28 (m, 1H), 7.17 (t, J = 9.6 Hz, 1H). ^{13}C NMR (150 MHz, DMSO-d_6) δ 164.21, 158.23, 156.54, 143.13, 136.21, 134.00, 133.47, 131.52, 130.39, 128.96, 128.04, 127.72, 127.51, 126.34, 125.62, 125.23, 125.17, 124.50, 122.26, 119.72, 119.61, 117.85, 116.80. ESI-HRMS [M − H]$^-$ calcd for $C_{23}H_{14}ClF_2NO_4S$: 472.0227, found: 472.0231.

*4.2.6. General procedure for the preparation of **E1**−**14***

To a solution of intermediate 10 (3.7 g, 11.03 mmol) in acetone (20 mL) was added methyl 2-(5-amino-2-fluorophenyl)acetate hydrochloride (1.94 g, 8.82 mmol) and pyridine (2.62g,

33.08 mmol). The mixture then was refluxed for 2 h and evaporated under vacuum. The residue was diluted with water and extracted with ethyl acetate (15 mL) three times. The combined ethyl acetate layer was sequentially washed with brine, dried with anhydrous Na_2SO_4, and concentrated to give the crude product. The crude was purified by column chromatography with petroleum/ethyl acetate to yield intermediate**12** as a prey solid (3.25 g, 61 %)

To a suspension of the intermediate **12** (1 equiv) in DMF (8 mL) was sequentially added appropriate substituted aryl boric acid (1.3 equiv), K_2CO_3 (2 equiv), $PdCl_2$ (dppf).CH_2Cl_2 (0.1 equiv) and water (0.5 mL). After refluxing for 12 h under N_2 atmosphere, the reaction mixture was cooled and then poured into H_2O. The mixture was extracted with extracted with EtOAc (2x), washed with saturated NaCl solution, dried over anhydrous Na_2SO_4, and concentrated in vacuo. The residue was purified by silica gel column chromatography to afford the target compounds as a white solid.(**13a-n**).

To a solution of intermediate 13a-n (1 equiv) in methanol (8 mL) was added 1 N NaOH solution (10 equiv) and stirred at room temperature for 1 h. Then the solvent was removed under vacuum, the residue was acidified to pH = 2 with HCl (1 M) solution and white solid precipitated. The mixture was extracted with ethyl acetate twice and the combined organic layer was dried over anhydrous sodium sulfate and concentrated to provide the target compounds as white solids E1-14.

*4.2.6.1. 2-(2-fluoro-5-((3-(4-fluoro-2-methylphenyl)-4-methoxynaphthalene)-1sulfonamido)phenyl) acetic acid (**E1**).* White solid, 71 %. ^{1}H NMR (400 MHz, DMSO-d_6) δ 12.47 (s, 1H), 10.66 (s, 1H), 8.74 (d, J = 8.4 Hz, 1H), 8.33–8.26 (m, 1H), 7.88 (s, 1H), 7.81 (d, J = 7.9 Hz, 1H), 7.75 (t, J = 7.6 Hz, 1H), 7.36–7.29 (m, 1H), 7.25 (d, J = 10.0 Hz, 1H), 7.20–7.12 (m, 1H), 7.02–6.97 (m, 2H), 6.90–6.86 (m, 1H), 3.52–3.45 (m, 5H), 1.99 (s, 3H). ^{13}C NMR (150 MHz, DMSO-d_6) δ 171.08, 162.45, 157.01, 156.41, 138.80, 133.35, 133.27, 132.75, 131.65, 128.82, 128.40, 128.24, 127.18, 125.61, 124.47, 123.18, 122.92, 120.26, 116.51, 115.44, 112.68, 61.16, 34.00, 19.35. ESI-HRMS [M − H]$^-$ calcd for $C_{26}H_{21}F_2NO_5S$: 496.1036, found: 496.1040.

*4.2.6.2. 2-(2-fluoro-5-((3-(4-fluorophenyl)-4-methoxynaphthalene)-1-sulfonamido)phenyl)acetic acid (**E2**).* White solid, 64 %. ^{1}H NMR (400 MHz, DMSO-d_6) δ 8.69 (d, J = 8.2 Hz, 1H), 8.28 (d, J = 8.1 Hz, 1H), 8.11 (s, 1H), 7.74–7.70 (m, 2H), 7.65–7.61 (m, 2H), 7.35 (t, J = 8.6 Hz, 2H), 7.05–7.03 (m, 1H), 6.98 (t, J = 9.2 Hz, 1H), 6.91–6.87 (m, 1H), 3.53 (s, 3H), 3.48 (s, 2H). ^{13}C NMR (150 MHz, DMSO-d_6) δ 171.20, 162.48, 157.93, 156.82, 133.39, 132.70, 132.37, 131.00, 130.95, 130.08, 128.56, 128.37, 128.32, 127.32, 126.25, 124.53, 123.14, 120.03, 119.98, 115.61, 115.46, 61.32, 34.14. ESI-HRMS [M − H]$^-$ calcd for $C_{25}H_{19}F_2NO_5S$: 482.0879, found: 482.0882.

*4.2.6.3. 2-(2-fluoro-5-((3-(2-fluorophenyl)-4-methoxynaphthalene)-1-sulfonamido)phenyl)acetic acid (**E3**).* White solid, 61 %. ^{1}H NMR (400 MHz, DMSO-d_6) δ 12.42 (s, 1H), 10.69 (s, 1H), 8.71 (d, J = 8.5 Hz, 1H), 8.29 (d, J = 8.3 Hz, 1H), 8.07 (s, 1H), 7.81 (t, J = 7.7 Hz, 1H), 7.74 (t, J = 7.6 Hz, 1H), 7.55–7.49 (m, 2H), 7.41–7.34 (m, 2H), 7.03–6.96 (m, 2H), 6.94–6.87 (m, 1H), 3.56 (s, 3H), 3.48 (s, 2H). ^{13}C NMR (150 MHz, DMSO-d_6) δ 171.11, 159.81, 157.94, 156.34, 133.25, 133.03, 131.57, 130.51, 129.41, 128.68, 128.62, 128.22, 127.31, 124.61, 124.51, 124.07, 123.22, 122.98, 122.82, 121.28, 119.97, 115.76, 115.48, 61.58, 34.02. ESI-HRMS [M − H]$^-$ calcd for $C_{25}H_{19}F_2NO_5S$: 482.0879, found: 482.0881.

*4.2.6.4. 2-(5-((3-(2-chlorophenyl)-4-methoxynaphthalene)-1-sulfonamido)-2-fluorophenyl)acetic acid (**E4**).* White solid, 57 %. ^{1}H NMR (400 MHz, DMSO-d_6) δ 12.44 (s, 1H), 10.69 (s, 1H), 8.72 (d, J = 8.5 Hz, 1H), 8.29 (d, J = 8.4 Hz, 1H), 7.97 (s, 1H), 7.81 (t, J = 7.7 Hz, 1H), 7.74 (t, J = 7.6 Hz, 1H), 7.69–7.63 (m, 1H), 7.55–7.47 (m, 3H), 7.02–6.94 (m, 2H), 6.90–6.86 (m, 1H), 3.53 (s, 3H), 3.46 (s, 2H). ^{13}C NMR (150 MHz, DMSO-d_6) δ 171.08, 157.94, 157.26, 135.44, 133.25, 132.35, 131.80, 130.02, 129.40, 128.84, 128.67, 128.55, 128.17, 127.22, 124.48, 124.45, 123.28, 122.93, 122.90, 119.97, 115.43, 61.39, 34.08. ESI-HRMS [M − H]$^-$ calcd for $C_{25}H_{19}ClFNO_5S$: 498.0584, found: 498.0585.

*4.2.6.5. 2-(2-fluoro-5-((4-methoxy-3-(2-(trifluoromethyl)phenyl) naphthalene)-1-sulfonamido) phenyl) acetic acid (**E5**).* White solid, 33 %. ^{1}H NMR (400 MHz, DMSO-d_6) δ 10.71 (s, 1H), 8.74 (d, J = 8.6 Hz, 1H), 8.26 (d, J = 8.3 Hz, 1H), 7.95 (s, 1H), 7.91 (d, J = 7.8 Hz, 1H), 7.84–7.69 (m, 4H), 7.54 (d, J = 7.5 Hz, 1H), 6.97–6.92 (m, 2H), 6.88–6.81 (m, 1H), 3.55 (s, 3H), 3.44 (s, 2H). ^{13}C NMR (150 MHz, DMSO-d_6) δ 171.09, 157.91, 156.98, 135.07, 133.17, 132.77, 132.43, 132.18, 128.86, 128.68, 128.56, 127.88, 127.31, 126.24, 124.95, 124.54, 123.34, 122.89, 122.75, 119.81, 115.33, 61.50, 34.00. ESI-HRMS [M − H]$^-$ calcd for $C_{26}H_{19}F_4NO_5S$: 532.0847, found: 532.0849.

*4.2.6.6. 2-(2-fluoro-5-((4-methoxy-3-(o-tolyl)naphthalene)-1-sulfonamido)phenyl)acetic acid (**E6**).* White solid, 84 %. ^{1}H NMR (400 MHz, DMSO-d_6) δ 12.45 (s, 1H), 10.63 (s, 1H), 8.72 (d, J = 8.7 Hz, 1H), 8.28 (d, J = 8.4 Hz, 1H), 7.87 (s, 1H), 7.79 (t, J = 7.9 Hz, 1H), 7.74 (d, J = 8.0 Hz, 1H), 7.39–7.35 (m, 2H), 7.33–7.29 (m, 1H), 7.25 (d, J = 7.2 Hz, 1H), 7.02–6.95 (m, 2H), 6.91–6.84 (m, 1H), 3.45 (s, 5H), 1.98 (s, 3H). ^{13}C NMR (150 MHz, DMSO-d_6) δ 171.07, 158.01, 156.78, 136.54, 135.72, 133.42, 133.30, 129.93, 129.69, 128.69, 128.29, 128.26, 128.08, 127.11, 126.44, 125.77, 124.44, 123.17, 123.13, 120.21, 115.44, 61.06, 34.04, 19.31. ESI-HRMS [M − H]$^-$ calcd for $C_{26}H_{19}F_4NO_5S$: 478.1130, found:4 78.1126.

*4.2.6.7. 2-(5-((3-(2-ethylphenyl)-4-methoxynaphthalene)-1-sulfonamido)-2-fluorophenyl)acetic acid (**E7**).* White solid, 58 %. ^{1}H NMR (400 MHz, DMSO-d_6) δ 12.46 (s, 1H), 10.64 (s, 1H), 8.75 (d, J = 8.6 Hz, 1H), 8.28 (d, J = 8.3 Hz, 1H), 7.87 (s, 1H), 7.81 (t, J = 7.8 Hz, 1H), 7.74 (t, J = 7.6 Hz, 1H), 7.40 (d, J = 9.1 Hz, 2H), 7.31 (d, J = 7.1 Hz, 1H), 7.25 (d, J = 7.6 Hz, 1H), 6.98 (d, J = 7.4 Hz, 2H), 6.86 (d, J = 8.9 Hz, 1H), 3.49 (s, 3H), 3.45 (s, 2H), 2.33–2.27 (m, 2H), 0.86 (t, J = 7.8 Hz, 3H). ^{13}C NMR (150 MHz, DMSO-d_6) δ 171.05, 158.05, 156.66, 141.67, 135.96, 133.53, 133.22, 129.84, 128.66, 128.30, 128.21, 127.14, 126.50, 125.71, 124.48, 123.41, 123.19, 122.93, 120.24, 115.40, 61.22, 34.04, 25.49, 14.51. ESI-HRMS [M − H]$^-$ calcd for $C_{27}H_{24}FNO_5S$: 492.1286, found: 492.1284.

*4.2.6.8. 2-(2-fluoro-5-((4-methoxy-3-(2-(trifluoromethyl)phenyl) naphthalene)-1-sulfonamido) phenyl) acetic acid (**E8**).* White solid, 61 %. ^{1}H NMR (400 MHz, DMSO-d_6) δ 12.45 (s, 1H), 10.64 (s, 1H), 8.74 (d, J = 8.5 Hz, 1H), 8.28 (d, J = 8.3 Hz, 1H), 7.87 (s, 1H), 7.83–7.78 (m, 1H), 7.74 (t, J = 7.5 Hz, 1H), 7.48–7.42 (m, 2H), 7.29 (t, J = 7.0, 1H), 7.21 (d, J = 7.6 Hz, 1H), 6.99–6.93 (m, 2H), 6.87–6.83 (m, 1H), 3.50 (s, 3H), 3.44 (s, 2H), 2.58–2.52 (m, 1H), 1.13–1.11 (m, 3H), 0.90–0.88 (m, 3H). ^{13}C NMR (150 MHz, DMSO-d_6) δ 171.03, 158.06, 156.76, 146.31, 135.27, 133.53, 133.18, 129.80, 128.68, 128.54, 128.31, 128.18, 127.17, 126.60, 125.57, 125.40, 124.47, 123.52, 123.23, 122.90, 120.19, 115.38, 61.24, 34.01, 29.59, 24.21, 22.57. ESI-HRMS [M − H]$^-$ calcd for $C_{28}H_{26}FNO_5S$: 506.1443, found: 506.1439.

*4.2.6.9. 2-(2-fluoro-5-((3-(2-hydroxyphenyl)-4-methoxynaphthalene)-1-sulfonamido)phenyl)acetic acid (**E9**).* White solid, 86 %. ^{1}H NMR (400 MHz, DMSO-d_6) δ 12.42 (s, 1H),10.64 (s, 1H), 9.65 (s, 1H), 8.65 (d, J = 8.5 Hz, 1H), 8.26 (d, J = 8.3 Hz, 1H), 8.10 (s, 1H), 7.76–7.67 (m, 2H), 7.31–7.22 (m, 2H), 7.02–6.90 (m, 5H), 3.55 (s, 3H), 3.46 (s, 2H). ^{13}C NMR (150 MHz, DMSO-d_6) δ 171.17, 157.76, 157.22, 154.41, 134.74, 133.43, 130.89, 129.35, 128.41, 128.31, 128.04, 126.76, 124.29, 124.08, 123.59, 123.08, 122.86, 122.70, 119.51, 118.99, 115.73, 115.41, 60.84, 34.11. ESI-HRMS [M − H]$^-$ calcd for

$C_{25}H_{20}FNO_6S$: 480.0923, found: 480.0921.

*4.2.6.10. 2-(5-((3-(2,4-difluorophenyl)-4-methoxynaphthalene)-1-sulfonamido)-2-fluorophenyl) acetic acid (**E10**).* White solid, 72 %. ^{1}H NMR (400 MHz, DMSO-d_6) δ 12.43 (s, 1H), 10.70 (s, 1H), 8.71 (d, J = 8.5 Hz, 1H), 8.28 (d, J = 8.4 Hz, 1H), 8.06 (s, 1H), 7.81 (t, J = 7.6 Hz, 1H), 7.75 (t, J = 7.6 Hz, 1H), 7.61–7.55 (m, 1H), 7.45 (t, J = 9.8 Hz, 1H), 7.28–7.24 (m, 1H), 7.05–6.96 (m, 2H), 6.91–6.87 (m, 1H), 3.56 (s, 3H), 3.48 (s, 2H). ^{13}C NMR (150 MHz, DMSO-d_6) δ 171.13, 161.40, 157.93, 157.85, 133.23, 132.93, 132.78, 129.53, 128.75, 128.69, 128.18, 127.36, 124.54, 123.22, 122.96, 122.82, 120.59, 120.41, 119.99, 115.47, 111.91, 104.24, 61.66, 34.00. ESI-HRMS [M − H]$^-$ calcd for $C_{25}H_{18}F_3NO_5S$: 500.0785, found: 500.0781.

*4.2.6.11. 2-(5-((3-(2-chloro-4-fluorophenyl)-4-methoxynaphthalene)-1-sulfonamido)-2-fluoro phenyl) acetic acid (**E11**).* White solid, 76 %. ^{1}H NMR (400 MHz, DMSO-d_6) δ 12.43 (s, 1H), 10.69 (s, 1H), 8.73 (d, J = 8.6 Hz, 1H), 8.28 (d, J = 8.4 Hz, 1H), 7.95 (d, J = 1.3 Hz, 1H), 7.85–7.79 (m, 1H), 7.75 (t, J = 7.7 Hz, 1H), 7.67 (d, J = 8.8 Hz, 1H), 7.57–7.53 m, 1H), 7.38 (t, J = 8.5, Hz, 1H), 7.00–6.95 (t, J = 8.5 Hz, 2H), 6.89–6.85 (m, 1H), 3.54 (s, 3H), 3.46 (s, 2H). ^{13}C NMR (150 MHz, DMSO-d_6) δ 171.10, 162.48, 157.94, 157.47, 133.41, 133.25, 131.88, 128.96, 128.75, 128.63, 128.14, 127.28, 124.50, 123.72, 123.29, 122.95, 122.78, 120.02, 116.81, 115.43, 114.65, 61.49, 34.05. ESI-HRMS [M − H]$^-$ calcd for $C_{25}H_{18}ClF_2NO_5S$: 516.0490, found: 516.0486.

*4.2.6.12. 2-(5-((3-(3-chloro-4-fluorophenyl)-4-methoxynaphthalene)-1-sulfonamido)-2-fluoro phenyl) acetic acid (**E12**).* White solid, 60 %.^{1}H NMR (400 MHz, DMSO-d_6) δ 12.36 (s, 1H), 10.69 (s, 1H), 8.70 (d, J = 8.3 Hz, 1H), 8.29 (d, J = 8.1 Hz, 1H), 8.12 (s, 1H), 7.81–7.73 (m, 3H), 7.62–7.55 (m, 2H), 7.07–7.04 (m, 1H), 6.99 (t, J = 9.0 Hz, 1H), 6.93–6.89 (m, 1H), 3.57 (s, 3H), 3.50 (s, 2H). ^{13}C NMR (150 MHz, DMSO-d_6) δ 171.16, 157.96, 157.07, 156.35, 134.02, 133.27, 132.13, 130.90, 130.12, 129.80, 128.64, 128.55, 128.46, 127.43, 125.16, 124.52, 123.23, 123.08, 122.98, 120.12, 119.69, 117.16, 115.54, 61.62, 33.98. ESI-HRMS [M − H]$^-$ calcd for $C_{25}H_{18}ClF_2NO_5S$: 516.0490, found: 516.0485.

*4.2.6.13. 2-(5-((3-(3-chloro-2-fluorophenyl)-4-methoxynaphthalene)-1-sulfonamido)-2-fluoro phenyl) acetic acid (**E13**).* White solid, 63 %. ^{1}H NMR (400 MHz, DMSO-d_6) δ 12.43 (s, 1H), 10.70 (s, 1H), 8.72 (d, J = 8.5 Hz, 1H), 8.29 (d, J = 8.2 Hz, 1H), 8.09 (s, 1H), 7.82 (t, J = 7.7 Hz, 1H), 7.78–7.71 (m, 2H), 7.49 (t, J = 7.2 Hz, 1H), 7.39 (t, J = 8.0 Hz, 1H), 7.03–6.96 (m, 2H), 6.90–6.87 (m, 1H), 3.58 (s, 3H), 3.48 (s, 2H). ^{13}C NMR (150 MHz, DMSO-d_6) δ 171.14, 157.94, 157.88, 155.16, 133.20, 132.65, 130.66, 130.47, 129.65, 128.92, 128.85, 128.12, 127.45, 125.81, 125.49, 124.58, 123.28, 122.95, 120.52, 120.13, 119.95, 115.48, 61.92, 33.98. ESI-HRMS [M − H]$^-$ calcd for $C_{25}H_{18}ClF_2NO_5S$: 516.0490, found: 516.0484.

*4.2.6.14. 2-(5-((3-(2,5-dichlorophenyl)-4-methoxynaphthalene)-1-sulfonamido)-2-fluorophenyl) acetic acid (**E14**).* White solid, 78 %. ^{1}H NMR (400 MHz, DMSO-d_6) δ 12.44 (s, 1H), 10.69 (s, 1H), 8.73 (d, J = 8.6 Hz, 1H), 8.29 (d, J = 8.4 Hz, 1H), 7.96 (s, 1H), 7.83 (t, J = 7.7 Hz, 1H), 7.75 (t, J = 7.6 Hz, 1H), 7.69 (d, J = 8.5 Hz, 1H), 7.62–7.57 (m, 2H), 6.99–6.95 (m, 2H), 6.89–6.85 (m, 1H), 3.57 (s, 3H), 3.46 (s, 2H). ^{13}C NMR (150 MHz, DMSO-d_6) δ 171.07, 157.95, 157.36, 137.15, 133.19, 132.81, 131.65, 131.30, 131.00, 129.87, 129.07, 128.87, 128.76, 128.08, 127.33, 124.52, 123.47, 123.33, 123.00, 122.78, 120.02, 115.42, 61.69, 34.04. ESI-HRMS [M − H]$^-$ calcd for $C_{25}H_{18}Cl_2FNO_5S$: 532.0194, found: 532.0189.

4.3. In vitro FABPs inhibition assay

The methods for expression and purification of FABP4/FABP5/FABP3 were as previously described [39]. The inhibitory activities of the compounds against FABPs were evaluated using 1-anilinonapthalene 8-sulfonic acid (1, 8-ANS) displacement assay [32,41]. Briefly, 1, 8-ANS (10 μM, diluted in phosphate buffered solution) was mixed with FABPs protein to a final concentration of 10 μM. The compounds were then added and incubated for 3 min at room temperature. The fluorescence signal at 370 nm (excitation)/470 nm (emission) was measured with a Flexstation III instrument (Molecular Devices, CA, USA). Compounds with inhibition rate greater than 60% at the concentration of 25 μM were selected for IC_{50} values determination.

4.4. Cell viability assay

Mouse 3T3-L1 preadipocytes and human THP-1 cells were from the American Type Culture Collection and were cultured as previously described [23,42]. For cell viability assay, 3T3-L1 cells were seeded in 96-well plates at the density of 6000 cells/well and then treated with fresh medium with or without 100 μM of compounds for 24 h. THP-1 cells were seeded in 96-well plates at the density of $1*10^5$ cells/well and simultaneously incubated with 100 nM of phorbol myristic acid (PMA) for 24 h to facilitated the differentiation to a macrophage phenotype. The cells were then treated with or without 50 μM of compounds for another 24 h. Appropriate concentrations of DMSO in medium was used as control. After that, the cell viability was assessed by using Cell Counting Kit-8 (CCK-8) according to manufacturer's instructions. Briefly, the original medium was discarded and 100 μl CCK-8 (10 %, v/v) reagent was added gently and incubated for 30 min at 37 °C. The absorbance was then read at 450 nm. Cell viability was calculated by (compound-treated group absorbance value/control group absorbance value) × 100 %.

4.5. Lipolysis assay

3T3-L1 preadipocytes were seed in 150 mm * 25 mm Dish for differentiation as previously described [42]. The mature adipocytes were digested by trypsin and seeded into 96-well plates at a density of 40000 cells/well and then incubated with compounds with various concentrations or DMSO (final concentration 0.1 %, v/v) for 24 h. On the day of lipolysis measurement, the cells were incubated in Krebs-Ringer-HEPES buffer with or without 20 μM forskolin for 1 h. Thereafter, the concentrations of glycerol in supernatants were measured using a commercial glycerol assay kit (Applygen Technologies Inc, China).

4.6. FABP4 secretion assay and western blotting

The mature adipocytes were starved in DMEM containing 0.5% BSA for 6 h, and then treated with 50 μM compound for 24 h. Supernatant was then collected for ultrafiltration while intracellular proteins were collected. Protein concentration of cell lysate and supernatant were determined by a bicinchoninic acid kit (Beyotime, China). Approximate 50 mg of liver tissues were lysed in RIPA Lysis Buffer (Beyotime, China) and the supernatant was collected after centrifugation (Eppendorf, Germany) as previously described [43]. Samples were then subjected to 10% or 12% SDS-PAGE, transferred to a 0.45 μm PVDF membrane, incubated with 1 % BSA and then probed with primary antibodies (FABP4 antibody, 2120, GAPDH, 5174, Akt antibody, 9272, phospho-Akt antibody, 9271, CST, USA, 1:1000 dilution) at 4 °C overnight. The next day, the PVDF membranes were washed with 1*TBST for 3 times and incubated with peroxidase-conjugated AffiniPure goat anti-rabbit

IgG (211-032-171, Jackson Laboratory, USA, 1:10000 dilution) for 90 min at room temperature. GAPDH was used as the loading control. The bands were visualized using ECL detection reagent (Thermo Fisher Scientific), and the intensity of the bands was quantified by using Gel-Pro Analyzer software.

4.7. RNA isolation and quantitative RT-PCR

THP-1 cells were seeded into 48-well plates at the density of $3*10^5$ cells/well and incubated with 100 nM PMA simultaneously for 24 h. After differentiated into macrophages, THP-1 cells were washed with PBS for three times gently. Compounds at the concentration of 25 μM or DMSO (final concentration 0.1 %, v/v) was added and incubated for 18 h followed by 100 ng/ml LPS stimulation for another 6 h. Total RNA was extracted from THP-1 cells using the TRIzol reagent (Invitrogen, USA) according to the manufacturer's instructions. Reverse transcription was performed by using All-in-One cDNA Synthesis SuperMix (Biomake, China) and the expression level of MCP-1 was quantified by real-time PCR with SYBR Green qPCR Master Mix (Biomake, China) and ABI VIIA7 Real-Time PCR machine (Applied Biosystems, USA). β-Actin was used as control. The relative expression level of MCP-1 was calculated using the $2^{-\Delta\Delta CT}$ method [32]. The primers used for RT-qPCR were listed as Table S1.

4.8. Metabolic stability in liver microsomes

Microsomes in 0.1 M TRIS buffer pH 7.4 (final concentration 0.33 mg/mL), co-factor $MgCl_2$ (final concentration 5 mM) and tested compound (final concentration 0.1 μM, co-solvent (0.01% DMSO) and 0.005% Bovin serum albumin (BSA)) were incubated at 37 °C for 10 min. The reaction was started by the addition of NADPH (final concentration 1 mM). Aliquots were sampled at 0, 7, 17, 30 and 60 min respectively and methanol (cold in 4 °C) was added to terminate the reaction. After centrifugation (4000 rpm, 5 min), samples were then analyzed by LC-MS/MS.

4.9. In vivo PK study in ICR (CD-1) mice

Eighteen ICR male mice were randomly divided into six group, weighting 20–25 g each. Compound **D9**, **E1** and **BMS309403** dissolved in phosphate-buffered saline containing 5% DMSO, and 0.5% hydroxypropyl methylcellulose (HPMC) was administered orally at a dose 3 mg/kg to three groups of mice. Another three groups of mice were injected with a single dose (1 mg/kg) of compound **E1**, **D9** and **BMS309403** which are dissolved in DMSO/ethanol (EtOH)/PEG300/NaCl (5/5/40/50, v/v/v/v). Blood samples at seven time points (0.25, 0.5, 1.0, 2.0, 4.0, 8.0, and 24 h) were collected. Plasma concentrations of compound **D9**, **E1** and **BMS309403** were analyzed by LC-MS/MS (Waters I-class LC system and Waters Xevo TQ-S Mass Spectrometer System).

4.10. Animal study

Male C57BL/KsJ-db/db mice and their lean littermates C57BL/KsJ-db/m mice were obtained from Jackson Laboratories (Bar Harbor, ME, USA) and kept in a light-dark cycle (12 h–12 h) at the temperature of 23 °C with regular chow diet and free access to water. To investigate the anti-diabetic effect of **D9** and **E1**, 6-week-old male *db/db* mice were divided into four groups ($n = 10$/group) and were given vehicle (0.5% sodium carboxyl methyl cellulose, CMC-Na), **D9** (50 mg/kg of body weight), **E1** (50 mg/kg of body weight) or **BMS309403** (50 mg/kg of body weight) by intragastric administration daily for 8 weeks, while their lean littermates were treated with vehicle in the same way. During administration, body weight was recorded twice a week. The mice were fasted for 6 h, and the blood glucose in the tail vain was monitored using a glucose meter once a week (Accu-CHEK, Roche). The oral glucose tolerance test (OGTT) and insulin tolerance test (ITT) were performed as previously described [43]. After 45 days of administration, the mice were fasted overnight and then were given 0.5 g/kg glucose *via* intragastric administration for OGTT. After 51 days of administration, the mice were subjected to insulin (0.85 IU/kg) *via* intraperitoneal injection after 6-h fasting for ITT. The line chart of blood glucose was plotted and the AUC were calculated. At the end of the experiment, blood samples were collected after the mice were fasted for 6 h and the serum parameters were determined using assay kit according to the manufacturer's instructions (Jiancheng, Nanjing, Chin; Biovendor, Brno, Czech Republic), including high density lipoprotein cholesterol (HDL-C), low density lipoprotein cholesterol (LDL-C), triglyceride (TG), total cholesterol (TCH) and FABP4. All animal experiments were permitted by the Institutional Animal Care and Use Committee of Shanghai Institute of Materia Medica (number: 2020-04-WHY-17).

4.11. Statistical analysis

The IC_{50} values of compounds for FABPs were calculated by nonlinear regression using GraphPad Prism software (San Diego, CA, USA) and expressed as mean ± standard deviation (SD) of three independent experiments. Statistical significance of different groups was performed by *t*-test or one-way analysis of variance (ANOVA) followed by a post hoc Tukey's test and a *p* value less than 0.05 was considered significant.

Declaration of competing interest

The authors declare that they have no known competing financial interests or personal relationships that could have appeared to influence the work reported in this paper.

Acknowledgements

The authors appreciate the financial support from the National Natural Science Foundation of China (81973178, 81773576), National Key R&D Program of China (2018YFC0310905); the "Personalized Medicines-Molecular Signature-based Drug Discovery and Development", Strategic Priority Research Program of the Chinese Academy of Sciences (XDA12040336).

Appendix A. Supplementary data

Supplementary data to this article can be found online at https://doi.org/10.1016/j.ejmech.2021.113720.

References

[1] U. Galicia-Garcia, A. Benito-Vicente, S. Jebari, A. Larrea-Sebal, H. Siddiqi, K.B. Uribe, H. Ostolaza, C. Martín, Pathophysiology of type 2 diabetes mellitus, Int. J. Mol. Sci. 21 (2020).
[2] R.L. Thomas, S. Halim, S. Gurudas, S. Sivaprasad, D.R. Owens, IDF Diabetes Atlas: a review of studies utilising retinal photography on the global prevalence of diabetes related retinopathy between 2015 and 2018, Diabetes Res. Clin. Pract. 157 (2019) 107840.
[3] M.C. Petersen, G.I. Shulman, Mechanisms of insulin action and insulin resistance, Physiol. Rev. 98 (2018) 2133–2223.
[4] C.M. Sena, C.F. Bento, P. Pereira, R. Seiça, Diabetes mellitus: new challenges and innovative therapies, EPMA J. 1 (2010) 138–163.
[5] M. Furuhashi, G.S. Hotamisligil, Fatty acid-binding proteins: role in metabolic diseases and potential as drug targets, Nat. Rev. Drug Discov. 7 (2008) 489–503.
[6] G.S. Hotamisligil, D.A. Bernlohr, Metabolic functions of FABPs–mechanisms and therapeutic implications, Nat. Rev. Endocrinol. 11 (2015) 592–605.
[7] G.S. Hotamisligil, R.S. Johnson, R.J. Distel, R. Ellis, V.E. Papaioannou,

B.M. Spiegelman, Uncoupling of obesity from insulin resistance through a targeted mutation in aP2, the adipocyte fatty acid binding protein, Science 274 (1996) 1377–1379.
[8] K.T. Uysal, L. Scheja, S.M. Wiesbrock, S. Bonner-Weir, G.S. Hotamisligil, Improved glucose and lipid metabolism in genetically obese mice lacking aP2, Endocrinology 141 (2000) 3388–3396.
[9] L. Scheja, L. Makowski, K.T. Uysal, S.M. Wiesbrock, D.R. Shimshek, D.S. Meyers, M. Morgan, R.A. Parker, G.S. Hotamisligil, Altered insulin secretion associated with reduced lipolytic efficiency in aP2$^{-/-}$ mice, Diabetes 48 (1999) 1987–1994.
[10] W.J. Shen, K. Sridhar, D.A. Bernlohr, F.B. Kraemer, Interaction of rat hormone-sensitive lipase with adipocyte lipid-binding protein, P. Natl. Acad. Sci. USA. 96 (1999) 5528–5532.
[11] L. Makowski, J.B. Boord, K. Maeda, V.R. Babaev, K.T. Uysal, M.A. Morgan, R.A. Parker, J. Suttles, S. Fazio, G.S. Hotamisligil, M.F. Linton, Lack of macrophage fatty-acid-binding protein aP2 protects mice deficient in apolipoprotein E against atherosclerosis, Nat. Med. 7 (2001) 699–705.
[12] M.A. Simpson, V.J. LiCata, N. Ribarik Coe, D.A. Bernlohr, Biochemical and biophysical analysis of the intracellular lipid binding proteins of adipocytes, Mol. Cell. Biochem. 192 (1999) 33–40.
[13] K. Maeda, K.T. Uysal, L. Makowski, C.Z. Görgün, G. Atsumi, R.A. Parker, J. Brüning, A.V. Hertzel, D.A. Bernlohr, G.S. Hotamisligil, Role of the fatty acid binding protein mal1 in obesity and insulin resistance, Diabetes 52 (2003) 300–307.
[14] A. Xu, Y. Wang, J.Y. Xu, D. Stejskal, S. Tam, J. Zhang, N.M. Wat, W.K. Wong, K.S. Lam, Adipocyte fatty acid-binding protein is a plasma biomarker closely associated with obesity and metabolic syndrome, Clin. Chem. 52 (2006) 405–413.
[15] J.B. Boord, K. Maeda, L. Makowski, V.R. Babaev, S. Fazio, M.F. Linton, G.S. Hotamisligil, Combined adipocyte-macrophage fatty acid-binding protein deficiency improves metabolism, atherosclerosis, and survival in apolipoprotein E-deficient mice, Circulation 110 (2004) 1492–1498.
[16] A. Josephrajan, A.V. Hertzel, E.K. Bohm, M.W. McBurney, S.I. Imai, D.G. Mashek, D.H. Kim, D.A. Bernlohr, Unconventional secretion of adipocyte fatty acid binding protein 4 is mediated by autophagic proteins in a sirtuin-1-dependent manner, Diabetes 68 (2019) 1767–1777.
[17] L.E. Wu, D. Samocha-Bonet, P.T. Whitworth, D.J. Fazakerley, N. Turner, T.J. Biden, D.E. James, J. Cantley, Identification of fatty acid binding protein 4 as an adipokine that regulates insulin secretion during obesity, Mol. Metab. 3 (2014) 465–473.
[18] H. Cao, M. Sekiya, M.E. Ertunc, M.F. Burak, J.R. Mayers, A. White, K. Inouye, L.M. Rickey, B.C. Ercal, M. Furuhashi, G. Tuncman, G.S. Hotamisligil, Adipocyte lipid chaperone AP2 is a secreted adipokine regulating hepatic glucose production, Cell Metabol. 17 (2013) 768–778.
[19] V. Lamounier-Zepter, C. Look, J. Alvarez, T. Christ, U. Ravens, W.H. Schunck, M. Ehrhart-Bornstein, S.R. Bornstein, I. Morano, Adipocyte fatty acid-binding protein suppresses cardiomyocyte contraction: a new link between obesity and heart disease, Circ. Res. 105 (2009) 326–334.
[20] M. Furuhashi, S. Saitoh, K. Shimamoto, T. Miura, Fatty acid-binding protein 4 (FABP4): pathophysiological insights and potent clinical biomarker of metabolic and cardiovascular diseases, Clin. Med. Insights Cardiol. 8 (2014) 23–33.
[21] M. Furuhashi, I. Sakuma, T. Morimoto, Y. Higashiura, A. Sakai, M. Matsumoto, M. Sakuma, M. Shimabukuro, T. Nomiyama, O. Arasaki, K. Node, S. Ueda, Treatment with anagliptin, a DPP-4 inhibitor, decreases FABP4 concentration in patients with type 2 diabetes mellitus at a high risk for cardiovascular disease who are receiving statin therapy, Cardiovasc. Diabetol. 19 (2020) 89.
[22] M. Furuhashi, T. Mita, N. Moniwa, K. Hoshina, S. Ishimura, T. Fuseya, Y. Watanabe, H. Yoshida, K. Shimamoto, T. Miura, Angiotensin II receptor blockers decrease serum concentration of fatty acid-binding protein 4 in patients with hypertension, Hypertens. Res. 38 (2015) 252–259.
[23] M. Furuhashi, G. Tuncman, C.Z. Gorgun, L. Makowski, G. Atsumi, E. Vaillancourt, K. Kono, V.R. Babaev, S. Fazio, M.F. Linton, R. Sulsky, J.A. Robl, R.A. Parker, G.S. Hotamisligil, Treatment of diabetes and atherosclerosis by inhibiting fatty-acid-binding protein aP2, Nature 447 (2007) 959–965.
[24] H. Su, Y. Zou, G. Chen, H. Dou, H. Xie, X. Yuan, X. Zhang, N. Zhang, M. Li, Y. Xu, Exploration of fragment binding poses leading to efficient discovery of highly potent and orally effective inhibitors of FABP4 for anti-inflammation, J. Med. Chem. 63 (2020) 4090–4106.
[25] H. Kuhne, U. Obst-Sander, B. Kuhn, A. Conte, S.M. Ceccarelli, W. Neidhart, M.G. Rudolph, G. Ottaviani, R. Gasser, S.S. So, S. Li, X. Zhang, L. Gao, M. Myers, Design and synthesis of selective, dual fatty acid binding protein 4 and 5 inhibitors, Bioorg. Med. Chem. Lett 26 (2016) 5092–5097.
[26] B. Buettelmann, S. M. Ceccarelli, A. Conte, H. Kuehne, B. Kuhn, W. Neidhart, U. Obst Sander, H. Richter, Urea Derivatives as Fatty-Acid Binding Protein(fabp) Inhibitors and Their Preparation, Pharmaceutical Compositions and Use in the Treatment of Diseases,WO2014146995A1.
[27] H. B. Sun, H. Y. Wang, C. X. Wang, H. L. Yuan, L. S. Han, W. Z. Wu, H. X. Dou, M. T. Chen, C. W. Yang, Preparation of Indole Derivatives and Used as Preventing or Treating FABP4/5 Mediated Diseases, CN112028815A.
[28] B. Buettelmann, S. M. Ceccarelli, H. Kuehne, B. Kuhn, W. Neidhart, U. Obst Sander, H. Richter, New Bicyclic Thiophenylamide Compound, WO2013189841A1..
[29] B. Buettelmann, A. Conte, H. Kuehne, B. Kuhn, W. Neidhart, U. Obst Sander, H. Richter, New Bicyclic Pyridine Derivatives as Fatty Acid Binding Protein Inhibitors and Their Preparation, WO2014029723A1..
[30] H. Lan, C.C. Cheng, T.J. Kowalski, L. Pang, L. Shan, C.C. Chuang, J. Jackson, A. Rojas-Triana, L. Bober, L. Liu, J. Voigt, P. Orth, X. Yang, G.W. Shipps Jr., J.A. Hedrick, Small-molecule inhibitors of FABP4/5 ameliorate dyslipidemia but not insulin resistance in mice with diet-induced obesity, J. Lipid Res. 52 (2011) 646–656.
[31] C. Look, I. Morano, M. Ehrhart-Bornstein, S.R. Bornstein, V. Lamounier-Zepter, BMS309403 directly suppresses cardiac contractile function, Naunyn-Schmiedeberg's Arch. Pharmacol. 384 (2011) 255–263.
[32] Y. He, H. Dou, D. Gao, T. Wang, M. Zhang, H. Wang, Y. Li, Identification of new dual FABP4/5 inhibitors based on a naphthalene-1-sulfonamide FABP4 inhibitor, Bioorgan, Med. Chem. 27 (2019) 115015.
[33] P. Lassalas, B. Gay, C. Lasfargeas, M.J. James, V. Tran, K.G. Vijayendran, K.R. Brunden, M.C. Kozlowski, C.J. Thomas, A.B. Smith III, D.M. Huryn, C. Ballatore, Structure property relationships of carboxylic acid isosteres, J. Med. Chem. 59 (2016) 3183–3203.
[34] B. Binas, H. Danneberg, J. McWhir, L. Mullins, A.J. Clark, Requirement for the heart-type fatty acid binding protein in cardiac fatty acid utilization, Faseb. J. 13 (1999) 805–812.
[35] A.V. Hertzel, K. Hellberg, J.M. Reynolds, A.C. Kruse, B.E. Juhlmann, A.J. Smith, M.A. Sanders, D.H. Ohlendorf, J. Suttles, D.A. Bernlohr, Identification and characterization of a small molecule inhibitor of Fatty Acid binding proteins, J. Med. Chem. 52 (2009) 6024–6031.
[36] N.R. Coe, M.A. Simpson, D.A. Bernlohr, Targeted disruption of the adipocyte lipid-binding protein (aP2 protein) gene impairs fat cell lipolysis and increases cellular fatty acid levels, J. Lipid Res. 40 (1999) 967–972.
[37] L. Makowski, K.C. Brittingham, J.M. Reynolds, J. Suttles, G.S. Hotamisligil, The fatty acid-binding protein, aP2, coordinates macrophage cholesterol trafficking and inflammatory activity. Macrophage expression of aP2 impacts peroxisome proliferator-activated receptor gamma and IkappaB kinase activities, J. Biol. Chem. 280 (2005) 12888–12895.
[38] T. Fuseya, M. Furuhashi, S. Yuda, A. Muranaka, M. Kawamukai, T. Mita, S. Ishimura, Y. Watanabe, K. Hoshina, M. Tanaka, K. Ohno, H. Akasaka, H. Ohnishi, H. Yoshida, S. Saitoh, K. Shimamoto, T. Miura, Elevation of circulating fatty acid-binding protein 4 is independently associated with left ventricular diastolic dysfunction in a general population, Cardiovasc. Diabetol. 13 (2014) 126.
[39] K.J. Prentice, J. Saksi, G.S. Hotamisligil, Adipokine FABP4 integrates energy stores and counterregulatory metabolic responses, J. Lipid Res. 60 (2019) 734–740.
[40] W.H. Lin, X.L. Huang, L.N. Zhang, D.M. Chen, D.Y. Wang, Q.L. Peng, L. Xu, J.Y. Li, X.J. Liu, K. Li, K. Ding, S.G. Jin, J. Li, D.H. Wu, BMS309403 stimulates glucose uptake in myotubes through activation of AMP-activated protein kinase, PloS One 7 (2012), e44570.
[41] H. Cai, G. Yan, X. Zhang, O. Gorbenko, H. Wang, W. Zhu, Discovery of highly selective inhibitors of human fatty acid binding protein 4 (FABP4) by virtual screening, Bioorg. Med. Chem. Lett 20 (2010) 3675–3679.
[42] H.Y. Cai, T. Wang, J.C. Zhao, P. Sun, G.R. Yan, H.P. Ding, Y.X. Li, H.Y. Wang, W.L. Zhu, K.X. Chen, Benzbromarone, an old uricosuric drug, inhibits human fatty acid binding protein 4 in vitro and lowers the blood glucose level in db/db mice, Acta Pharmacol. Sin. 34 (2013) 1397–1402.
[43] D.D. Gao, H.X. Dou, H.X. Su, M.M. Zhang, T. Wang, Q.F. Liu, H.Y. Cai, H.P. Ding, Z. Yang, W.L. Zhu, Y.C. Xu, H.Y. Wang, Y.X. Li, From hit to lead: structure-based discovery of naphthalene-1-sulfonamide derivatives as potent and selective inhibitors of fatty acid binding protein 4, Eur. J. Med. Chem. 154 (2018) 44–59.